Scalar Coupling between the ^{15}N Centres in Methylated 1,8-Diaminonaphthalenes and 1,6-Diazacyclodecane: To What Extent is $^{2H}J_{NN}$ a Reliable Indicator of N–N Distance?

Guy C. Lloyd-Jones,*[a] Jeremy N. Harvey,*[a] Paul Hodgson,[b] Martin Murray,[a] and Robert L. Woodward[a]

Abstract: The scalar couplings between hydrogen bonded nitrogen centres ($^{2H}J_{NN}$) in the free-base and protonated forms of the complete series of [$^{15}N_2$]-*N*-methylated 1,8-diamino naphthalenes in [D_7]DMF solution have been determined, either directly ($^{15}N\{^1H\}$ NMR), or, indirectly ($^{13}C\{^1H\}$ NMR and simulation of the X part of the ABX spectrum (X = ^{13}C, A,B = ^{15}N)). Additionally, the $^{2H}J_{NN}$ value in the HBF_4 salt of [$^{15}N_2$]-1,6-dimethyl-1,6-diazacyclodecane was determined, indirectly by $^{13}C\{^1H\}$ NMR spectroscopy. As confirmed by DFT calculations and by reference to CSD, the rigid nature of the naphthalene scaffold results in rather low deviations in N,N distance or H-N,N angle within each series, apart from the free base of the permethylated compound (proton sponge) where the naphthalene ring is severely distorted to relieve strain. Despite such restrictions, the $^{2H}J_{NN}$ values increase smoothly from 1.5 to 8.5 Hz in the protonated series as the degree of methylation increases. The effect in the free-base forms is much less pronounced (2.9 to 3.7 Hz) with no scalar N,N coupling detected in the permethylated compound (proton sponge) due to the lack of hydrogen bond between the N,N centres. Neither the pK_a nor the N–N distance in the protonated forms correlates with $^{2H}J_{NN}$. However, the sum of the ^{13}C NMR shifts of the naphthalene ring C(1,8) carbons which are attached directly to the nitrogen centres correlates linearly with $^{2H}J_{NN}$ and with the degree of methylation. The gas-phase computed $^{2H}J_{NN}$ is almost constant throughout the homologous series, and close to the experimental value for the tetramethylated ion. However, the computed coupling constant is attenuated in structures involving microsolvation of each N-H unit, and the trend then matches experiment. These experimental and computational observations suggest that Fermi contact between the two N centres is decreased upon formation of strong charge-dispersing intermolecular hydrogen bonds of the free N-H groups with the solvent.

Keywords: density functional calculations · hydrogen bonds · NMR spectroscopy · solvent effects · spin–spin coupling

Introduction

Hydrogen bonding is a structural feature that is ubiquitous and yet essentially peerless. As a crucial element in structural and chemical control, its study remains an area of intense interest and activity. There is an enormous diversity of hydrogen bonded/bonding species with a very broad spectrum of strength and (a)symmetry.[1] Hydrogen bond "strength" may be crudely broken down into three ranges. Those classed as "strong" may be generalised as a predominantly covalent interaction with a bond energy in the range 10–40 kcal mol^{-1}, whilst "moderate" are in the range 4–10 kcal mol^{-1} and "weak" are below 4 kcal mol^{-1} and predominantly arise from electrostatic interactions. "Low-barrier hydrogen bonds" (LBHB) and "short-strong hydrogen bonds"(SSHB), are two types of hydrogen bond that are often misleadingly considered as one and the same. Their potential involvement[2, 3] in the massive rate accelerations effected by enzymic catalysis is an area that continues to attract vigorous debate.[4] The arguments for[2] and against[3] both the existence and the relevance of such interactions have often been based on analogy with much simpler non-biological systems that can be more fully analysed and characterised. Since most examples of strong hydrogen bonds occur in species that are in the gas-phase, solution-phase examples are much sought after. *N*-Methylated 1,8-diaminonapthalenes (**1**–**6**) provide an inter-

[a] Dr. G. C. Lloyd-Jones, Dr. J. N. Harvey, Dr. M. Murray, Dr. R. L. Woodward
The School of Chemistry, University of Bristol
Cantock's Close, Bristol BS8 1TS (UK)
Fax: (+44) 117-929-8611
E-mail: guy.lloyd-jones@bris.ac.uk
jeremy.harvey@bris.ac.uk

[b] Dr. P. Hodgson
Pfizer Central Research
Ramsgate, Sandwich, CT13 9NJ (UK)

 DOI: 10.1002/chem.200304890

esting series of compounds for study. The hydrogen bond in $[\mathbf{6}H]^+$, the protonated form of archetypal first generation[5] proton sponge[6] **6**, has been suggested as a solution phase example of a LB/SS-HB. Indeed the hydrogen bond strength in $[\mathbf{6}H]^+$ has been proposed by Gerlt, Kreevoy, Cleland and Frey to be as high as 15 kcal mol^{-1}.[4]

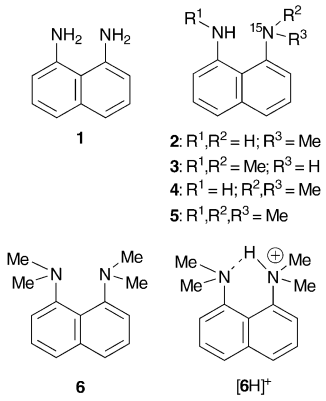

This latter conclusion is based on the surprisingly low acidity of $[\mathbf{6}H]^+$ ($pK_a > 18$ in MeCN; > 12 in H_2O) as compared to, for example, $[Ph\text{-}N(H)Me_2]^+$ which is approximately a million-fold more acidic. However, it is noted that $[\mathbf{1}H]^+ - [\mathbf{5}H]^+$, which all contain the potential for analogous intramolecular hydrogen bonding, are much more acidic (pK_a 11 – 13 in MeCN) than $[\mathbf{6}H]^+$. This feature,[3] as well as the study of N-stereodynamics[7] and isotopic perturbation[8] has led others to question such conclusions about both the strength and the symmetry of the hydrogen bond in $[\mathbf{6}H]^+$. The unusual properties of first generation proton sponges such as **6** have also attracted the attention of computational chemists.[9–12] Most calculations suggest the presence of an unusually strong hydrogen bond in $[\mathbf{6}H]^+$. However, it is noted that these calculations are generally conducted "in the gas phase" in the absence of solvation.

New tools for the characterisation of hydrogen bonds are particularly valuable and NMR has proved an abundant source.[13] It is therefore not surprising that the recent observation and measurement of scalar coupling constants[14] across hydrogen-bonded nitrogen centres in Watson – Crick base pairs by Dingley and Grzesiek[14, 15] and Pervushin et al.,[16] has caused much interest. These couplings are represented as "$^{2H}J_{NN}$" and are most often measured in ^{15}N-H-^{15}N systems.[14] Based on DFT calculations, Limbach et al. have proposed that in contrast to "normal" hydrogen bonds between two nitrogen centres where a maximum $^{2H}J_{NN}$ value of about 10 Hz is observed, symmetrical hydrogen bonds (LBHB) should display the maximum value of about 25 Hz.[17] In search for an example of an N-H-N hydrogen bond displaying the latter characteristics, Limbach et al., chose to determine the $^{2H}J_{NN}$ value in $[\mathbf{6}H]^+$, on the basis that the proton sponge system contains an "already classical intramolecular low-barrier $[N\cdots H\cdots N]^+$ hydrogen bond".[18] However, the $^{2H}J_{NN}$ value in $[^{15}N_2]$-$[\mathbf{6}H][ClO_4]$ was determined as 8.7 ($\pm$0.5) Hz whilst $[^{15}N_2]$-[**6**], which lacks the N-H-N unit, displayed no detectable J_{NN} (0 ($\pm$0.5) Hz). Both determinations were made indirectly by ^{13}C NMR spectroscopy, using a multiple frequency-based approach that involved spectra being acquired on 250, 500 and 750 MHz (^1H frequency) spectrometers.[18]

Results and Discussion

Recent developments in computation suggest that genuine information on hydrogen bond "strength", geometry, symmetry and, in particular donor-acceptor distance (r_{NN}) in "N-H$\cdots$N" systems is available through determination of the NMR coupling constant between the N centres.[15, 17, 19–21] This coupling is suggested to arise predominantly by Fermi-contact between the N centres *through* the H-bond and is thus represented as "$^{2H}J_{NN}$". We have an ongoing interest in the hydrogen bonding in first generation proton sponges.[5] Our thermodynamic data, derived from comparison of the kinetics of stereodynamic processes in *N*,*N*′-dibenzyl-*N*,*N*′-dimethyl-1,8-diaminonaphthalene[22, 23] with its protonated form[7] led us to conclude that the hydrogen bond in the protonated form, and thus by analogy in $[\mathbf{6}H]^+$, is not of any unusual enthalpic strength or special "character". To further study these species, we have prepared a number of ^{15}N labelled 1,8-diaminonaphthalenes so that we can determine experimental values for $^{2H}J_{NN}$ in such systems. Whilst we were engaged in these studies, the $^{2H}J_{NN}$ value for $[^{15}N_2]$-$[\mathbf{6}H][ClO_4]$, see above, was published.[18] Herein we report on the synthesis and determination of $^{2H}J_{NN}$ values for the protonated and free base forms of the *non*-permethylated compounds in the series (**1** – **5**) as well as the proton sponge compound **6**. We also demonstrate that it is not necessary to make measurements at different fields in order to determine the $^{2H}J_{NN}$ scalar coupling in formally symmetrical N-H-N systems by ^{13}C NMR spectroscopy and also that the ABX method is *not* "limited to compounds exhibiting sufficiently large ^{13}C isotope effects $\Delta^{15}N\{^{13}C\}$ on the nitrogen chemical shifts".[18] We use the $^{2H}J_{NN}$ data in three distinct ways. Firstly we compare the experimentally determined $^{2H}J_{NN}$ values with known pK_a values (of the protonated forms)[24] and reinforce earlier conclusions regarding the "normality" of hydrogen bonding between the N centres in the protonated form of the archetypal bis-*N*,*N*′-(dialkyl)-1,8-diaminonaphthalene proton sponge compounds. Secondly, in response to the suggestion of Del Bene that the predicted dominance of the Fermi-contact term (and thus N,N distance and the H-N,N angle) in determining $^{2H}J_{NN}$ be tested experimentally[20] we have performed DFT calculations to establish equilibrium intramolecular N,N distance (r_{NN}) and H-N,N angles (a_{NHN}) in all 12 species (**1** – **6** and $[\mathbf{1}H]^+ - [\mathbf{6}H]^+$). The r_{NN} values arising from these DFT calculations, which are likely to be close to the time-averaged values, compare well with average values in the solid state established by survey of the Cambridge Structural Database (CSD). Finally, we have calculated $^{2H}J_{NN}$ for all 12 species (**1** – **6** and $[\mathbf{1}H]^+ - [\mathbf{6}H]^+$), which has led us to consider how this coupling constant is affected by factors other than N,N distance (r_{NN}) and H-N,N angles (a_{NHN}), especially intermolecular hydrogen bonding.

Synthesis of the full homologous series of *N*,*N*′-(methyl)$_n$-1,8-diamino naphthalenes ($n = 0$ to 4) in [^{15}N$_2$]-labelled form: Generation of the complete series [^{15}N$_2$]-**1** to [^{15}N$_2$]-**6** involved the preparation of [^{15}N$_2$]-**1** by reduction of [^{15}N$_2$]-1,8-dinitronaphthalene ([^{15}N$_2$]-**7**) and then a controlled, that is, non exhaustive, methylation of [^{15}N$_2$]-**1**, as had been conducted with **1** by Alder et al. in their seminal work on (unlabelled) **6**.[5] Using a combination of two equivalents Na^{15}NO$_3$[25] in a solvent mixture of $(CF_3CO_2)O/CF_3CO_2H/CHCl_3$, to effect a one-pot double nitration[26] we obtained [^{15}N$_2$]-**7** in 31.4% yield with [^{15}N$_2$]-1,5-dinitronaphthalene (13% yield) as the major side product in addition to a range of other mono- and poly-nitronaphthalene isomers. The desired dinitro species [^{15}N$_2$]-**7** was separated by crystallisation, hydrogenated to give 1,8-diamine [^{15}N$_2$]-**1** (87%) and then the bulk of [^{15}N$_2$]-**1** was methylated (NaH/MeI) in a one-pot, two-step, sequence. The use of 2.0 equivalents MeI was found to give the optimum distribution of products, which were separated by gradient elution from alumina, to give [^{15}N$_2$]-**2** (26%) [^{15}N$_2$]-**3**[27] (4%), [^{15}N$_2$]-**4** (14%) and [^{15}N$_2$]-**5** (43%) in an overall yield of 96% (based on MeI), Scheme 1. A titration of [^{15}N$_2$]-**5** in [D$_7$]DMF with ethereal hydrogen iodide,[28] monitored by ^{1}H NMR

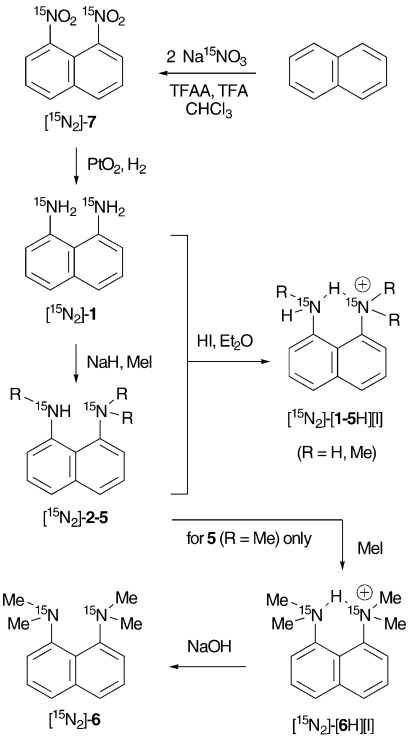

Scheme 1. Outline of the synthetic route used to prepare ^{15}N labelled compounds [^{15}N$_2$]-**1**–[^{15}N$_2$]-**6**, and [^{15}N$_2$]-[**1**H][I]–[^{15}N$_2$]-[**6**H][I] (>90% ^{15}N$_2$; <7.5% ^{15}N$_1$; <2.5% ^{15}N$_0$) from Na^{15}NO$_3$ (> 95% ^{15}N) and naphthalene. Note that compounds [^{15}N$_2$]-**2**–**5** were isolated as separate species and then protonated to give [^{15}N$_2$]-[**2**][I]–[**5**H][I] as separate species.

(chemical shift and half-peak line width of the NMe$_2$ unit) demonstrated that proton exchange between [^{15}N$_2$]-[**5**H][I] and [^{15}N$_2$]-**5** is rapid and also that use of excess HI (up to 2 equiv) gave no evidence for double protonation. Preparative mono-protonation gave the HI salts [^{15}N$_2$]-[**1**H][I], [^{15}N$_2$]-[**2**H][I], [^{15}N$_2$]-[**3**H][I], [^{15}N$_2$]-[**4**H][I] and [^{15}N$_2$]-[**5**H][I] in quantitative yields.

Neutral methylation[23] of trimethyl diamine [^{15}N$_2$]-**5** was readily achieved by its dissolution in MeI, from which [^{15}N$_2$]-[**6**H][I] crystallised in 77% yield. Deprotonation (NaOH) afforded [^{15}N$_2$]-**6** (91%), a small sample of which was re-protonated with TfOH to give [^{15}N$_2$]-[**6**H][OTf] so that the effect of counterion (I^- versus ClO_4^-,[18] versus TfO^-) on $^{2H}J_{NN}$ could be probed.

Determination of $^{2H}J_{NN}$ values by direct and indirect methods: For the purpose of determination of the $^{2H}J_{NN}$ values by ^{13}C and ^{15}N NMR spectroscopy (Table 1), the samples were dissolved in dry, degassed [D$_7$]DMF. The non-symmetrical free base and protonated species ([^{15}N$_2$]-**2**, [^{15}N$_2$]-**4**, [^{15}N$_2$]-**5** and [^{15}N$_2$]-[**2**H][I], [^{15}N$_2$]-[**4**H][I], [^{15}N$_2$]-[**5**H][I]) displayed well-resolved AX systems (all of the $\Delta\delta$N (Hz)/$^{2H}J_{NN}$ values lie within the range 329 to 20) in their ^{15}N{^{1}H} NMR spectra from which the $^{2H}J_{NN}$ values were determined directly by standard means (Table 1.

The time-average symmetrical species ([^{15}N$_2$]-**1**, [^{15}N$_2$]-**3**,[27] [^{15}N$_2$]-**6** and [^{15}N$_2$]-[**1**H][I], [^{15}N$_2$]-[**3**H][I],[27] [^{15}N$_2$]-[**6**H][I]) were studied by ^{13}C{^{1}H} NMR, focusing in particular on C(1,8). At ambient temperature these carbons are degenerate at the NMR time scale and form the X part of an AA′X spin system which is desymmetrised by the net isotope shift of the ^{13}C (observed nucleus, C(1)) versus the ^{12}C (99% non-observed nucleus, C(8)) to an ABX spin system (see experimental section for full discussion). Full band shape analysis of the X-part of the spectrum [using the parameters J_{AB} ($= J_{NN'}$); J_{AX} ($= J_{CN}$); J_{BX} ($= J_{CN'}$); $\tilde{\nu}_A$; $\tilde{\nu}_B$ ($\tilde{\nu}_A - \tilde{\nu}_B = \Delta\delta$ ^{15}N, the isotope shift); $\tilde{\nu}_X$ and the natural line-width $\omega_{0.5}$; see Table 3 in Experimental Section] allowed extraction of the $^{2H}J_{NN}$ value (J_{AB}) (Table 1) for each compound from a single spectrum. This differs from the frequency-based approach employed earlier, which requires a number of spectra be acquired, each at different fields.[18] The simulations were found to be sensitive to variations in all of the parameters, each parameter giving a unique response, thus allowing acceptable confidence limits to be established. In the upper section of Figure 1, systematic variations (A–E) in the parameters J_{AB}, J_{AX}, J_{BX}, $(\tilde{\nu}_A - \tilde{\nu}_B)$[29] and $\omega_{0.5}$ for the simulation of the C(1,8) signal for [^{15}N$_2$]-**6**H][I] are shown. Set C in each series is the best-fit. Some other examples of best-fit simulations superimposed with real spectra are given in the lower section.

Considering the $^{2H}J_{NN}$ values for the free base (**2**–**6**, open circles in Figure 2)) and protonated forms ([**2**–**6**H]$^+$, filled circles in Figure 2), both show a trend of increasing $^{2H}J_{NN}$ with increasing degree of methylation. The increase in $^{2H}J_{NN}$ for the protonated form is strikingly smooth, covers a range of over 7 Hz and spans the much smaller range of 0.9 Hz observed in the free bases **1**–**5**. As has been suggested earlier, the unusually high basicity of **6**, as compared to **1**–**5**, is predominantly due to relief of strain on protonation and not due to any unusual properties of the H-bond in [**6**H]$^+$. Accordingly, the $^{2H}J_{NN}$ values for [**1**H]$^+$–[**6**H]$^+$ do not display a simple relationship with pK_a[30] or with the (time average) chemical shift of the hydrogen bonded proton. (Table 1).

Table 1. Selected NMR, physical and computational data[a] for neutral and protonated forms (HI) of diaminonaphthalenes **1**–**6** and the protonated form (HBF_4) of 1,6-dimethyl-1,6-diazacyclodecane, [**10**H]$^+$.

Species $(Me)_n$[b]	$\delta^{15}N$ [ppm][c]	$\delta^{13}C(1,8)$ [ppm]	$\delta^{1}H(N^+H)$ [ppm][d]	$^{2H}J_{NN}$[e] [Hz]	pK_a[f]	r_{NN}[g] [Å]	a_{NHN}[h] [°]	Σr_{NH}[i] [Å]
1 (0)	62.7,62.7	147.7,147.7	–	2.88 (0.3)	–[j]	2.716[k]	106.1	3.268
[**1**H]$^+$ (0)	62.1,62.1	133.2,133.2	9.36	1.5 (0.2)	10.99	2.598[l]	153.2	2.669
2 (1)	59.5,61.7	149.5,146.9	–	3.25(0.2)	–[j]	2.716	115.0	3.141
[**2**H]$^+$ (1)	47.1,48.4	132.5,135.1	8.85	2.6 (0.2)	11.64	2.644	151.8	2.722
3 (2)	52.4,52.4	149.2,149.2	–	3.21 (0.3)	–[j]	2.726	131.2	2.964
[**3**H]$^+$ (2)	37.8,37.8	133.7,133.7	8.43	–[m]	11.95	2.625	154.2	2.691
4 (2)	35.8,62.5	153.5,148.0	–	3.3 (0.2)	–[j]	2.739	125.8	3.032
[**4**H]$^+$ (2)	32.9,44.7	149.6,130.5	4.21	4.46 (0.2)	12.87	2.652	154.9	2.702
5 (3)	35.1,58.6	153.3,149.2	–	3.71 (0.2)	–[j]	2.719	133.9	2.930
[**5**H]$^+$ (3)	32.8,41.7	149.4,138.8	12.90	6.68 (0.2)	12.91	2.645	156.0	2.661
6 (4)	46.0,46.0	151.7,151.7	–	0 (0.5)[n]	–[j]	2.860[o]	–[p]	–[p]
[**6**H]$^+$ (4)	35.5,35.5	146.1,146.1	18.68	8.46(0.2)	18.18	2.617[q]	158.6	2.714
[**6**H]$^{+}$[r] (4)	34.9,34.9	146.0,146.0	18.66	8.80(0.2)	–[s]	2.617[q]	158.6	2.714
[**10**H]$^+$ (2)	42.9,42.9	–	19.51	10.56 (0.5)	>12[t]	2.602[t]	169[t]	2.62[t]

[a] NMR data from isotopically labelled compounds (>90 % $^{15}N_2$; <7.5 % $^{15}N_1$; <2.5 % $^{15}N_0$). [b] "*n*" is the number of methyl groups. [c] 40.6 MHz (400 ^{1}H) in [D_7]DMF with ^{1}H decoupling, chemical shift referenced against $NH_3 = 0$ ppm. [d] Proton chemical shifts in the non-permethylated compounds [**1**–**5**H]$^+$ are time-average values inclusive of chemical shifts arising from non-H-bonded protons with which they rapidly exchange at the NMR time scale. [e] Estimated errors in parenthesis, see experimental details. For (time-average) symmetrical species, $^{2H}J_{NN}$ determined by simulation of X part of ABX in ^{13}C NMR sub-spectrum. [f] pK_a, in MeCN, from ref. [24]. [g] Intramolecular N–N distance in lowest energy structure according to DFT calculation, see Experimental Section for full details. [h] The angle N-H-N of the hydrogen bond in the lowest energy structure according to DFT calculation, see Experimental Section for full details. [i] Sum of the two N–H distances in the intramolecular N-H-N hydrogen bond. [j] pK_a values are given for protonated forms only. [k] Average intramolecular N–N distance from 7 structural determinations of this compound deposited in the CSD is 2.73 Å. [l] Average intramolecular N–N distance from 7 structural determinations of the cationic fragment of this compound, irrespective of counterion, deposited in the CSD is 2.67 Å. [m] Not determined with sufficient accuracy, see ref. [27]. [n] No coupling detected. [o] Average intramolecular N–N distance from 3 structural determinations of this compound deposited in the CSD is 2.77 Å. [p] No hydrogen bond present due to permethylation. [q] Average intramolecular N–N distance from 67 structural determinations of the cationic fragment of this compound, irrespective of counterion, deposited in the CSD is 2.58 Å. [r] Counterion is triflate. [s] pK_a not determined for this salt. [t] From ref. [45], angles and lengths from X-ray structure of HI salt.

The strain in **6**, that induces its unusual basicity, arises from lone-pair/lone-pair repulsion. Partial relief of this strain is achieved by delocalisation of the lone pairs into the aromatic ring (requiring trigonalisation at N). However, this process is hindered by the resulting steric clash between *N* and *N*′-methyl groups and between methyl groups and the C(1,7)-H units. As a consequence of such clashes, some distortion of the aromatic ring arises, as is evident in single crystal X-ray structures. Analogous strain is not present in **1**–**5** due to the presence of one, or more, N-H units. The N-H unit imparts the ability of such species to form an intramolecular hydrogen bond and in doing so, trigonalise one N centre and delocalise the lone pair with the aromatic ring. It is this intramolecular hydrogen bond which in turn facilitates the $^{2H}J_{NN}$ coupling. Observation of significant J_{NN} coupling in **1**–**5** supports the presence of this hydrogen bonding which is not evident in the ^{1}H NMR spectrum due to time-average degeneracy of the N-H protons caused by exchange. The permethylation in **6** does not allow analogous hydrogen bonding and accordingly no J_{NN} coupling is detected[31] until it has been protonated to give [**6**H]$^+$.

Relationship of $^{2H}J_{NN}$ values to donor-acceptor distance (r_{NN}): A number of computational studies have been conducted on the relationship between $^{2H}J_{NN}$ and N,N distance (r_{NN}), NHN angles (a_{NHN}), N–H bond lengths (r_{NH}) N-hybridisation and charge in intermolecular [N-H···N] hydrogen-bond complexes.[19–21, 32–41] DFT calculations performed by Dingley et al. on internucleotide hydrogen bonds suggested a near-linear relationship between $^{2H}J_{NN}$ and r_{NN} when one r_{NH} value was held constant. The predicted values were found to correlate closely with the measured values for a G-C base pair when r_{NN} was assumed to be 2.92 Å and the N–H distance 1.038 Å.[15b] In contrast, high level ab initio calculations on a large and diverse range of complexes (neutral and anionic donors and neutral and cationic acceptors) by Del Bene[19, 20] predict that $^{2H}J_{NN}$ values should correlate smoothly, but non-linearly, with r_{NN}, providing that the [N-H···N] unit is linear ($a_{NHN} = 180°$) and each complex is at its equilibrium r_{NN} geometry, see crosses in Figure 3.

For a given equilibrium r_{NN} value, the predicted $^{2H}J_{NN}$ value is not significantly affected by hybridisation or charge.[19] Furthermore, deliberate distortion of [N-H···N] units from linearity or displacement of the vector of the lone-pair on the donor away from co-linearity with the hydrogen bond were both found to have a minor effect on $^{2H}J_{NN}$ providing that such distortions were not extreme.[20] Analogously small (but opposite) effects were found for the isotropic component of $^{2H}J_{NN}$ by Bryce and Wasylishen for methyleneimine dimer.[21] Overall, such results have interpreted to suggest that the relationship between $^{2H}J_{NN}$ and r_{NN} "…will be useful for determining N–N distances from coupling constants measured in hydrogen-bonded complexes stabilized by either N-H-N or N-H$^+$-N hydrogen bonds…".[20] Limbach et al. have recently determined solution phase $^{2H}J_{NN}$ values for symmetric [$^{15}N_2$]-*N*,*N*′-diphenyl-6-aminopentafulvene-1-aldimine ([$^{15}N_2$]-**8**) and the non-symmetric [1,6-$^{15}N_2$]-*N*-phenyl-*N*′-(1,3,4-triazol)-6-aminopentafulvene-1-aldimine ([$^{15}N_2$]-**9**).[42] The $^{2H}J_{NN}$ value in the latter compound has also been determined as 7.3 Hz in the solid state.[43] Using r_{NN} values

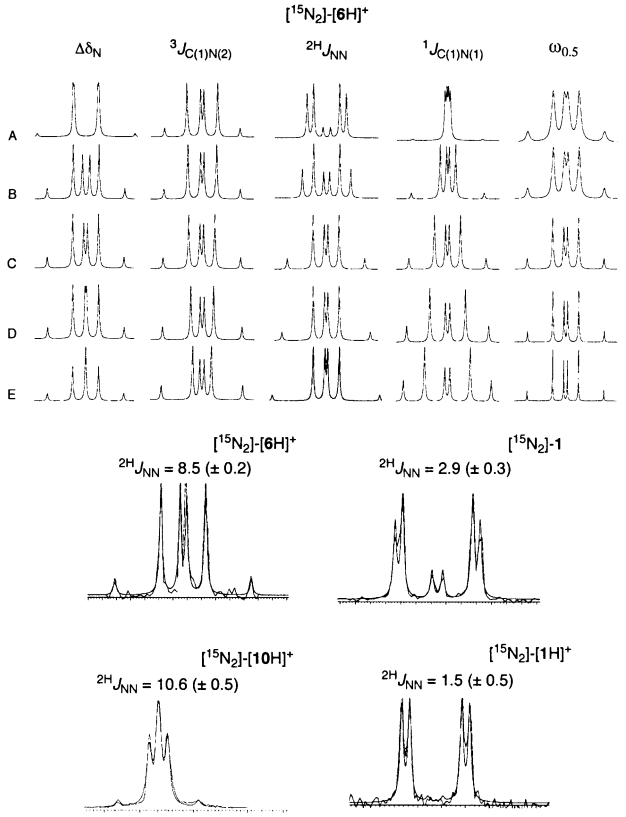

Figure 1. Simulations of X part of ABX spectra (X = ^{13}C, AB = ^{15}N). Upper section: the effect on the X spectrum when the five parameters $[\tilde{\nu}_A - \tilde{\nu}_B]$ (= $\Delta\delta_N$, the isotope shift); J_{BX} (= $^3J_{C(1)N(2)}$); J_{AB} (= $^{2H}J_{NN}$); J_{AX} (= $^1J_{C(1)N(1)}$) and $\omega_{0.5}$ (= the natural line-width) are varied independently with all other parameters locked at their best fit values. Five variations are shown (A to E) with set C corresponding to the parameters generating the best fit with the real spectrum [parameters for C: $\Delta\delta_N = 26$ ppb, $^3J_{C(1)N(2)} = 1.16$ Hz, $^{2H}J_{NN'} = 8.46$ Hz, $^1J_{C(1)N(1)} = -7.62$ Hz and $\omega_{0.5} = 0.4$ Hz]. Parameters for A, B, D and E are: $\Delta\delta_N$: 500, 50, 10 and 0; $^3J_{C(1)N(2)}$: 0, 0.5, 2 and 3; $^{2H}J_{NN}$: 2, 4, 10, 12.5; $^1J_{C(1)N(1)}$: −2.5, −5.0, −10.0, −12.5; $\omega_{0.5}$: 1, 0.75, 0.25, 0.15. Lower section: selected best fit simulations superimposed on the experimental ^{13}C{^{1}H} sub-spectra of [^{15}N$_2$]-[**6**H][I], [^{15}N$_2$]-[**10**H][BF$_4$], [^{15}N$_2$]-**1** and [^{15}N$_2$]-[**1**H][I] (see Table 3 for full details).

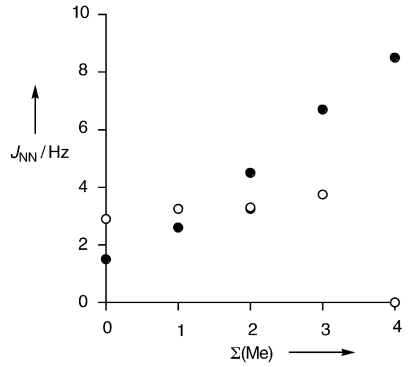

Figure 2. The smooth relationship between the degree of methylation (ΣMe) in the two series [^{15}N$_2$]-[**1**–**6**] (○) and [^{15}N$_2$]-[**1**–**6**H][I] (●) and the N,N coupling constant ($^{2H}J_{NN}$) in [D$_7$]DMF solution at 22 °C. For [^{15}N$_2$]-[**1**–**6**H][I], $^{2H}J_{NN}$/ Hz = 1.80 (±0.11) [Σ(Me)]+1.08 (±0.27).

taken from the CSD, it is apparent that the experimentally determined $^{2H}J_{NN}$ values for these intramolecularly hydrogen

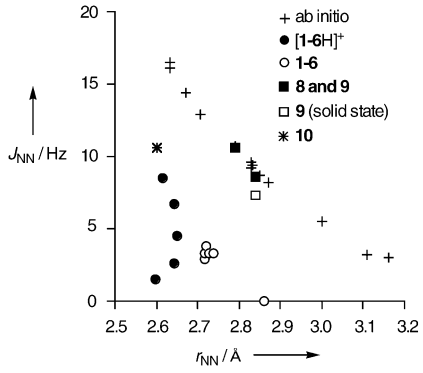

Figure 3. Graph of N,N coupling constant ($^{2H}J_{NN}$) at equilibrium N–N separation (r_{NN}). +: calculated values for a range of intermolecular hydrogen bonded complexes, data taken from refs. [19] and [20]. ●: [^{15}N$_2$]-[**1**–**6**H][I]. ○: [^{15}N$_2$]-**1**–**6** (note that J_{NN} for **6** is close to zero due to no hydrogen bond being present) both cases in [D$_7$]DMF solution with r_{NN} from DFT calculations. ■: [^{15}N$_2$]-**8** and [^{15}N$_2$]-**9** in CDCl$_3$ solution, r_{NN} for **8** and **9** from CSD, data from ref. [42]. □: [^{15}N$_2$]-**9** in solid state, data from ref. [43]. *: [^{15}N$_2$]-**10** in [D$_7$]DMF solution with r_{NN} from CSD, data from ref. [45].

bonded systems (squares, Figure 3) are remarkably close to those predicted from the curve derived from the calculations of Del Bene on intermolecular hydrogen bond complexes, despite non-linearity of the hydrogen bonds ($a_{NHN} = 154–155°$) in **8** and **9**.

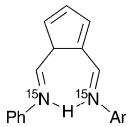

8: Ar = Ph
9: Ar = 1,3,4-triazole

We therefore sought to ascertain whether the trends in coupling constants in the species described here could be correlated with changes in r_{NN}. To do this, we have optimized gas-phase structures for **1**–**6** and [**1**H]$^+$–[**6**H]$^+$ using DFT (B3LYP level of theory, with the flexible 6-311G(d,p) basis set), selected data are given in Table 1. Based on previous computational studies of proton sponges,[9–12] this level of theory should provide reliable geometries. The geometries obtained are mostly unremarkable, and are in good agreement with those derived from previous Hartree–Fock[9, 10] and especially DFT[12] calculations. Two major factors determine the structures of the neutral species: rotation of the amine groups so as to relieve lone-pair repulsion, and formation of fairly weak hydrogen bonds between the two nitrogens (except in the permethylated compound **6**). In the protonated species, there is a reasonably strong hydrogen bond, leading also to a significantly shorter N–N distance in all cases. The structures have protons localised on one of the nitrogen atoms only, again in agreement with previous computational work and with experiment[8] although the barriers for intramolecular proton transfer are assumed to be low.

We have also conducted a survey of the CSD[44] and extracted the r_{NN} values from every report of any of these structures. It emerges that only **1**, [**1**H]$^+$[X]$^-$, **6** and [**6**H]$^+$[X]$^-$ (X = unspecified counterion) have been reported (the latter species some 71 times). The r_{NN} values derived from the DFT calculations agree satisfactorily with the CSD derived data and this confirms that the DFT derived r_{NN} values for the

intermediate species (**2**–**5**) and [**2**H]$^+$–[**5**H]$^+$ should be reasonably reliable. When the experimentally determined J_{NN} values for **1**–**6** (open circles) and [**1**H]$^+$-[**6**H]$^+$ (closed circles) are plotted against r_{NN} (Figure 3) it is readily apparent that they do not correlate with the predicted values. This lack of correlation is manifest both in significantly lower $^{2H}J_{NN}$ values than would be predicted for r_{NN} in the range 2.6–2.7 Å and also in the diversity of the $^{2H}J_{NN}$ values within such a small range of r_{NN}. Clearly, the rigidity of the N–C=C–C–N array means that r_{NN} is restricted to a very small range of values in these compounds, so that changes in N–N distance (r_{NN}) cannot account for the observed changes in coupling constants ($^{2H}J_{NN}$).

Analysis of the NHN angle suggests that, for the protonated species at least, insufficient deviation from linearity is present ($a_{NHN} = 152–159°$) to result in such a discrepancy with the predicted r_{NN} versus $^{2H}J_{NN}$ curve. Indeed, the a_{NHN} values are similar to those in **8** and **9** which correlate almost perfectly. The free base forms **1**–**5** display a wide range of significantly smaller angle ($a_{NHN} = 106–134°$) but in contrast display a much smaller range of $^{2H}J_{NN}$ values. In both series (free base and protonated), the observed $^{2H}J_{NN}$ values are significantly lower than would be expected from the "normal" trend in Figure 3. The hydrogen bonding in the protonated proton sponge species is sometimes referred to as being "under compression".[45] That is, the rigidity of the naphthalene scaffold results in a much lower r_{NN} value than there would be if the N-H-N unit *alone* were to control the equilibrium geometry in the absence of the constraints of the C–C bonded framework. However, compression and elongation of model systems predicts smooth relationships between r_{NN} versus predicted $^{2H}J_{NN}$ that mirrored the relationship arising from equilibrium r_{NN} values in the series of compounds.[20] In other words, non-equilibrium r_{NN} should still result in a reasonably predictable $^{2H}J_{NN}$ value. To probe whether a general medium effect may play an important factor, we re-performed the DFT calculations on the protonated series [**1**H]$^+$–[**6**H]$^+$ using a polarisable medium that mimics DMF. Consistent with the rigidity of the diaminonaphthalene system, there were only very slight changes in the structure. The most notable of these were a small elongation of the N–N distance (Δr_{NN} 0.001–0.050 Å) and a slight bending of the N-H-N unit further away from linearity (Δa_{NHN} 0.8–4.8°) as the medium was changed from the gas phase to a DMF mimic. However, these changes are far too small to decrease the deviation between predicted and observed $^{2H}J_{NN}$ to a significant extent.

Relationship between $^{2H}J_{NN}$ values and inductive effects on the naphthalene ring: The restriction in the current two systems (**1**–**6** and [**1**H]$^+$–[**6**H]$^+$) to small variations in r_{NN}, provides an opportunity to explore in an isolated manner other factors that must therefore contribute to the magnitude of $^{2H}J_{NN}$. The smooth increase in $^{2H}J_{NN}$ in the series [**1**H]$^+$–[**6**H]$^+$ suggests that the increasing degree of methylation directly or indirectly increases the Fermi contact, the dominant contributor to the coupling,[19–21] between the N centres. In both series, the naphthalene ring is a constant, whilst the degree of methylation is variable and we thus chose to use [$\Sigma^{13}C_{1,8}$], the sum of the ^{13}C shifts of C(1) and C(8) (see Table 1) normalised against naphthalene,[46] as a probe for the inductive effects arising as a consequence of the electronic interaction between the naphthalene ring and the {R_2N-H-NR_2} unit to which it is bound through the C(1) and C(8) carbons. In such a manner we find that the $^{2H}J_{NN}$ coupling is related both to the degree of methylation in the series **1**–**5** and [**1**H]$^+$–[**6**H]$^+$ (Figure 2) and also to [$\Sigma^{13}C_{1,8}$], where a good correlation is observed (Figure 4).

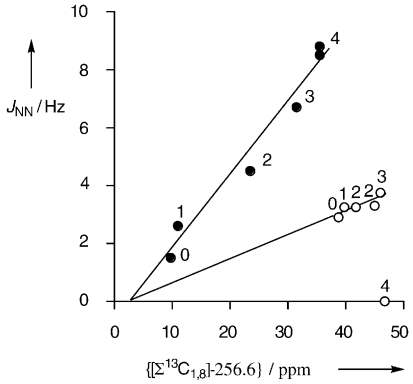

Figure 4. Graph of the N,N coupling ($^{2H}J_{NN}$ for all but **6**) in [$^{15}N_2$]-**1**–**6** and [$^{15}N_2$]-[**1**–**6**H][I] in [D$_7$]DMF against the sum of the C(1) and C(8) chemical shifts, normalised against the chemical shift of naphthalene. Open circles are for [$^{15}N_2$]-**1**–**6;** filled circles are for [$^{15}N_2$]-[**1**–**6**H][I]. Data taken from Table 1. The labels (0 to 4) above data-points are the number of methyl groups in each species. Straight lines passing through data-points are linear regressions of the two data sets (excluding the free base form of **6** for which $^{2H}J_{NN}$ is zero). For [$^{15}N_2$]-[**1**–**6**H][I], $^{2H}J_{NN} = 0.24(\pm0.03)[\Sigma^{13}C_{1,8})\text{-}256.6] - 0.6(\pm0.6)$; for [$^{15}N_2$]-**1**–**5** $^{2H}J_{NN} = 0.081(\pm0.3)[\Sigma^{13}C_{1,8}) - 256.6] - 0.1(\pm1.2)$.

Considering the data, it is evident that as the degree of methylation is increased (see Σ(Me) associated with data points in Figure 4) the electron demand on the ring is strongly modulated in the protonated series ($\Delta\Sigma^{13}C_{1,8}$ ca. 27 ppm) with a similar but much smaller trend in the neutral series ([$\Delta\Sigma^{13}C_{1,8}$] ca. 8 ppm). Initially this result in the cationic series, [**1**H]$^+$–[**6**H]$^+$, may appear contra-intuitive: a methyl group should be more electron donating (inductive) than a hydrogen, and increasing methylation would therefore be expected to stabilise the N-cationic centres, reduce the net electron withdrawing effect of the {R_2N-H-NR_2} unit and thus *decrease* the [$\Delta\Sigma^{13}C_{1,8}$] value. The opposite effect is observed, see above. However, concomitant with increasing methylation is, of course, a parallel decrease in the number of non *intra*molecularly hydrogen bonded N-H units. Intermolecular hydrogen bonding of these N-H units would be rather favourable in the protonated forms since this would delocalise the positive charge of the ammonium centre. A consequence of this would be a reduction in the charge localised at the N-centres and thus a reduction in the net electron withdrawing effect exerted at C(1,8) of the naphthalene ring. Considering first [**1**H]$^+$, which has the opportunity to engage in four separate intermolecular hydrogen bonding interactions, a stepwise increase in methylation (in the series [**1**H]$^+$–[**6**H]$^+$) should then result in a stepwise decrease in charge delocalisation. This would then be accompanied by a stepwise increase in demand for electron donation by the naphthalene ring and thus an increasing [$\Delta\Sigma^{13}C_{1,8}$] value.

In addition to the *variation* of the $^{2H}J_{NN}$ values within the series [**1**H]$^+$–[**6**H]$^+$, there also remains the issue of the large deviation of even the maximum $^{2H}J_{NN}$ value (ca. 8.5 Hz) with that predicted by consideration of the computed curve for model systems in Figure 3. Based on the discussion above, we wondered whether this deviation might be due to peculiarities in the electronic structure of these naphthyl diamines, associated with the inductive effects within the C–N bond, or to a more general polarisation of the naphthyl ring by the ammonium substituent. To answer this, we have also studied the double ^{15}N labelled HBF_4 salt of *N*,*N*′-dimethyl-1,6-diazacyclodecane (**10**),[47, 48] and measured the $^{2H}J_{NN}$ value of this purely aliphatic *in*-protonated diamine.

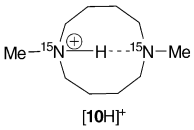

[**10**H]$^+$

The time-average symmetry of this species again involved the analysis of the X-part of an ABX spin system in the ^{13}C{^{1}H} NMR spectrum and using this technique the $^{2H}J_{NN}$ was determined as 10.6 Hz. The hydrogen bond assembly in this system is close to linearity ($a_{NHN} = 169°$) and is time-average symmetrical in both the solid state (X-ray) and solution (NMR). The observation that a similar deviation between r_{NN} NMR-predicted and NMR-observed $^{2H}J_{NN}$ also occurs in this fully aliphatic transannular hydrogen-bonded cationic N-H-N system, see asterisk in Figure 3, strongly supports the notion that the naphthalene ring is not responsible for the analogously large deviations in the series [**1**H]$^+$–[**6**H]$^+$ and **1** to **5**.

Computation of N,N-Fermi-contacts for 1–6 and [1H]$^+$–[6H]$^+$ and the effect of microsolvation: So as to gain further insight into the origin of the variation in $^{2H}J_{NN}$ for the 1,8-diaminonaphthalenes, and especially their protonated forms [**1**H]$^+$–[**6**H]$^+$, we also used DFT (with the ADF program package,[49] using the standard BP86 functional as B3LYP calculations cannot be performed with this program) to calculate the coupling constants. First, we ensured that this method (BP86 computation of $^{2H}J_{NN}$ at the B3LYP geometry) gives results similar to those obtained for example by Del Bene et al.[19, 20] Our computed values for three cases spanning the range from "weak" to "strong" coupling are indeed in good agreement with previous computed values: $^{2H}J_{NN}$ is found to be respectively 2.7, 5.0 and 8.9 Hz for the pyrrole–HNC, CNH–NCH and CNH–pyridine complexes, as compared with values of 3.0, 5.5 and 10.7 Hz computed at the CCSD-EOM ab initio level of theory. For the CNH–NCH complex, we obtained a strong dependence of $^{2H}J_{NN}$ with respect to r_{NN} when the latter is changed from its equilibrium value, as in ref. [19].

Next, we computed $^{2H}J_{NN}$ coupling constants for the free bases **1**–**6**. By and large, considering that our calculations treat isolated gas-phase species, the results are in excellent agreement with experiment (see Table 2, entries 1–6).

In contrast, analogous computations in the protonated series [**1**H]$^+$–[**6**H]$^+$ significantly over-estimated the coupling for all but [**6**H]$^+$. Indeed, as with the free-base series, the computed couplings were essentially independent of the degree of methylation (Table 2, entries 7–12). We considered several possible reasons for this discrepancy with experiment. First, our calculations are carried out at the equilibrium geometry, whereas the observed coupling constants arise from averaging over the range of configurations sampled on the NMR time scale. For example, NMR measurements on the protonated forms [**1**H]$^+$, [**3**H]$^+$ and [**6**H]$^+$ show the two nitrogens to be identical, whereas the equilibrium computed structure corresponds to a desymmetrised structure with the proton associated with one nitrogen only. This is due to the low barrier to intramolecular proton transfer. Del Bene et al. have shown[37] that the effective coupling constants obtained as ensemble averages of the computed values at specific geometries can be significantly different from the equilibrium value. In the present case, the "most different" geometry likely to be sampled at thermal energies is the transition state for intramolecular proton transfer, and we have accordingly recomputed $^{2H}J_{NN}$ at this geometry for [**1**H]$^+$ and [**6**H]$^+$. As might be expected from the fact that this structure involves much stronger electronic coupling between the two amine functions, the $^{2H}J_{NN}$ at this point is somewhat larger than that at the unsymmetric equilibrium geometry: 9.3 versus 7.5 Hz for [**1**H]$^+$, and 8.5 versus 6.7 for [**6**H]$^+$. Vibrational averaging of this type may therefore account in part for the fact that the computed coupling constant for [**6**H]$^+$ is somewhat smaller than the experimental value. However, even taking into account the fact that averaging will also involve some geometries where $^{2H}J_{NN}$ is lower than at the equilibrium position, it seems extremely unlikely that the low values of $^{2H}J_{NN}$ for [**1**H]$^+$–[**5**H]$^+$ could be explained in this way.

The most likely remaining explanation for the very significant deviation of the measured coupling constants of these ions from the simple correlation with r_{NN} is solvent effects, and especially hydrogen bonding by "free" N-H groups to the electron rich carbonyl group of DMF. This

Table 2. The observed and computed $^{2H}J_{NN}$values [a] for the free-base and the protonated, cationic forms of diaminonaphthalenes **1**–**6**.

	Species (Me)$_n$[c]	$^{2H}J_{NN}$ observed[b] [Hz]	$^{2H}J_{NN}$ calculated [Hz] in gas phase	with N-H micro-solvation[d]
1	**1** (0)	2.88 (0.3)	3.34	
2	**2** (1)	3.25(0.2)	3.46	
3	**3** (2)	3.21 (0.3)	3.51[e]	
4	**4** (2)	3.3 (0.2)	2.77	
5	**5** (3)	3.71 (0.2)	3.62	
6	**6** (4)	0 (0.5)	0.32[f]	
7	[**1**H]$^+$ (0)	1.5 (0.2)	7.53	4.37
8	[**2**H]$^+$ (1)	2.6 (0.2)	6.31	4.81
9	[**3**H]$^+$ (2)	–[g]	5.85	–[h]
10	[**4**H]$^+$ (2)	4.46 (0.2)	6.85	6.04
11	[**5**H]$^+$ (3)	6.68 (0.2)	6.17	6.51
12	[**6**H]$^+$ (4)	8.46(0.2)	6.67	–[i]

[a] The coupling between N,N centres through the intramolecular hydrogen bond, except for entry 6. [b] NMR data from isotopically labelled compounds (> 90 % $^{15}N_2$; < 7.5 % $^{15}N_1$; < 2.5 % $^{15}N_0$). Calculated data from DFT (BP86) calculations, see Experimental Section for full details. [c] "*n*" is the number of methyl groups. [d] Each non-intramolecularly hydrogen bonded N-H unit in the *cationic* series has a DMF molecule added to mimic hydrogen bonding to the solvent. [e] For *trans* [D,L]-isomer. [f] Coupling mechanism is through space. [g] Not determined with sufficient accuracy, see ref. [27]. [h] Not calculated. [i] Not applicable (no non-intramolecularly hydrogen bonded N-H unit available).

hypothesis is not easy to probe by computation, as ADF is not able to compute coupling constants in the presence of continuum solvent.[50] In any case, the solvent effect will depend on the degree of charge transfer from the solute to the solvent within the hydrogen bond, and this interaction is not described by continuum models.[51]

So as to address this issue, we therefore chose to represent the solvent by considering equilibrium structures for $[\mathbf{1}H]^+$–$[\mathbf{5}H]^+$, microsolvated by one DMF molecule hydrogen bonding to each non-intramolecular H-bonded N-H. The optimized structure of the $[\mathbf{1}H]^+$ microsolvate is contrasted with that of the bare ion in Figure 5. These microsolvated structures[52] only provide a static snapshot of the dynamic solvent-solute interactions, and it is unclear that the restriction to one solvent molecule per N-H unit is justified. However, these models do give some interesting insight into the properties of $[\mathbf{1}H]^+$–$[\mathbf{5}H]^+$.[53]

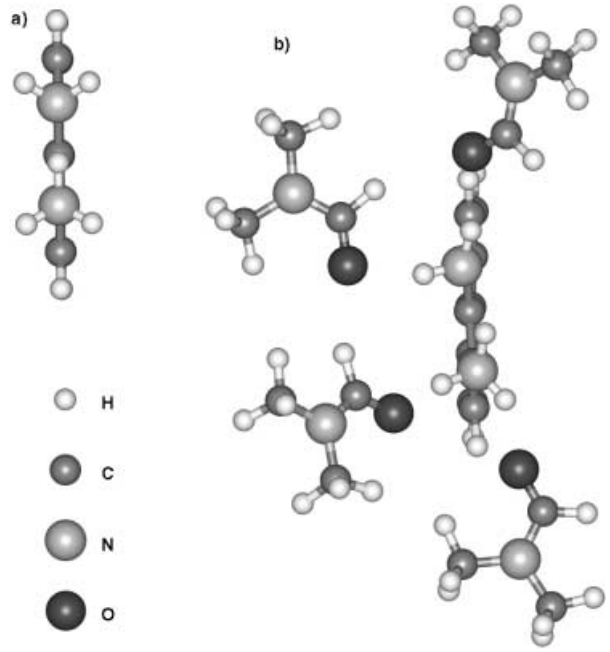

Figure 5. DFT optimised structures of bare $[\mathbf{1}H]^+$ (a) and of the $[\mathbf{1}H]^+ \cdot (DMF)_4$ microsolvate (b). For full discussion see text.

First, the optimised structures are considerably distorted from the gas-phase structures, with significant rotation around the C–N bond in most cases, leading to disrupted intramolecular hydrogen bonding but to more favourable solute–solvent interactions. Although r_{NN} and a_{NHN} do not change very significantly (in $[\mathbf{1}H]^+ \cdot (DMF)_4$, for example, r_{NN} increases to 2.671 from 2.598 Å in the bare ion, and a_{NHN} decreases from 153.2 to 136.8°), it can be seen in Figure 5 that the acceptor NH_2 group rotates quite significantly, so that the lone pair no longer points directly towards the donor NH_3^+ group. The fact that relatively weak hydrogen bonding to DMF can cause these changes in geometry of the main intramolecular hydrogen bond supports the previous conclusion[7] that hydrogen bonding in protonated diaminonapthalenes is not abnormally strong. Next, analysis of the wavefunctions of these microsolvates shows that there is indeed significant solute to solvent charge transfer. In $[\mathbf{1}H]^+ \cdot (DMF)_4$, the four solvent molecules have a total NBO[54] charge of +0.12. Compared to the gas-phase ion, the charge on the $[N_2H_5]^+$ moiety has barely changed (+0.53 vs +0.50), but the charge on the 1,8-naphthyl framework has markedly decreased, from +0.50 to +0.35. This charge transfer process thereby suggests that the observed increase in $[\Sigma^{13}C_{1,8}]$ upon increasing the degree of methyl substitution is indeed due to a decreased ability to hydrogen bond to solvent.

More significantly from the present point of view, the computed $^{2H}J_{NN}$ values for these microsolvates also agree much better with experiment than those derived from the gas phase structures. Thus, the spin–spin coupling was found to rise smoothly in the order $[\mathbf{1}H]^+$–$[\mathbf{5}H]^+$, Table 2, entries 7–11. It should be noted that the computed $^{2H}J_{NN}$ values remain larger than the experimental ones, but the crude nature of the microsolvation model means that exact numerical reproduction of the solvent effect is not expected. A significant part of the change in coupling constant is due to the disruption in the hydrogen-bonding geometry discussed above: the computed $^{2H}J_{NN}$ for the $[\mathbf{1}H]^+$ ion at its optimized geometry within the $[DMF]_4$ microsolvate but in the absence of the DMF molecules (5.5 Hz) is already much smaller than the value calculated at the equilibrium structure of this bare ion (7.5 Hz). Most of this change is probably due to the fact that the hydrogen bond acceptor lone pair is no longer optimially oriented towards the donor.

However, geometry changes alone do not explain the whole change in coupling, as the computed value for the distorted but unsolvated ion, 5.5 Hz, remains larger than that for the full solvated species (4.4 Hz). This further decrease in coupling must be due to *electronic* effects disrupting hydrogen bonding. Wilkens et al.[55] have found that NBO analysis can provide insight into the origin of spin–spin coupling constants. In the specific case of $^{2H}J_{NN}$ coupling, they found that delocalisation of the hydrogen-bond "acceptor" N lone pair into the antibonding N-H orbital of the hydrogen bond donor makes a large contribution to the computed $^{2H}J_{NN}$ in the adenine-thymine base pair.[55] NBO analysis[54] of $[\mathbf{1}H]^+$ and its microsolvated form indicates how solvation might affect spin–spin coupling between the two nitrogen nuclei. Thus, the key N lone pair–N-H σ* interaction is severely attenuated in the microsolvates: the N-H σ* has an NBO population of 0.14 electrons in the bare ion, mainly due to donation from the lone pair on the other nitrogen; this electron delocalisation interaction has an associated stabilisation energy $E(2)$ of 59.2 kcal mol^{-1} (this is related to but *not* identical to the overall stabilisation energy due to hydrogen bonding). These properties are very similar in bare $[\mathbf{6}H]^+$: 0.14 electrons in the N-H σ* orbital, and a lone pair–σ* delocalisation energy of 50.9 kcal mol^{-1}. In the $[DMF]_4$ solvate, the interaction is much weakened: the σ* orbital now only contains 0.06 electrons, and the orbital interaction stabilisation energy is only 19.7 kcal mol^{-1}. This reflects the lesser importance of N-H···N hydrogen bonding, with N-H···O=CH(NMe$_2$) interactions instead becoming of significant importance: the strongest such interaction, involving the bottom left-hand DMF molecule in Figure 5 and the corresponding N–H bond of the

NH_3^+ group, also leads to a σ* electron population of 0.06, and an orbital interaction stabilisation energy of 15.9 kcal mol^{-1}.

Overall, it is clear that solvation of non- or partially-methylated 1,8-diaminonaphthalene cations can have a strong effect on the magnitude of the intramolecular N,N spin–spin coupling. Solvation is a very complex phenomenon which is only partly described by the microsolvation model used here, so that it is not really possible to conclude whether the main effect on the coupling constants is due to the geometric or the electronic disruption created by hydrogen bonding to solvent.

Conclusion

In summary, we have prepared a range of neutral and cationic (protonated) diamine species in $^{15}N_2$-labelled form and performed DFT calculations to estimate geometries of hydrogen bonds, where present. The scalar NMR coupling between the nitrogen centres has been measured by two methods: one direct (^{15}N NMR) for the non-symmetrical species (**2**, **4**, **5**, [**2**H]$^+$, [**4**H]$^+$ and [**5**H]$^+$) and the other indirect (^{13}C NMR) for the time-average symmetrical species (**1**, **3**, **6**, [**1**H]$^+$, [**3**H]$^+$ [**6**H]$^+$ and [**10**H]$^+$). Smooth variations in the coupling constant in the series [**1**–**6**H]$^+$ suggests that the indirect method allows reliable extraction of J_{NN} from time-average symmetrical systems. In contrast to earlier techniques,[18] the method does not require a multiple frequency approach, or substantial isotope shifts, to be effective. Consistent with a) the presence of an intramolecular N-H-N hydrogen bond in all of the free base forms except **6**, b) the dominant coupling mechanism being Fermi-contact between N centres through the hydrogen bond (i.e., $^{2H}J_{NN}$) and c) very similar N–N separation (r_{NN}) in **1**–**5**, the coupling constant varies only slightly through the series **1**–**5** (2.8–3.7 Hz) but is 0 Hz in **6**. Nonetheless, the observed $^{2H}J_{NN}$ values are significantly lower than the values based on those predicted on the basis of DFT and ab initio calculations of the relationship between N–N separation (r_{NN}) and $^{2H}J_{NN}$ in model systems (see above). In the protonated series [**1**–**6**H]$^+$, the $^{2H}J_{NN}$ value spans some 7 Hz, despite similarly small variation in r_{NN}. Again, all values are significantly lower than the values predicted by the computated relationship between (r_{NN}) and $^{2H}J_{NN}$ in model systems. The modulation of $^{2H}J_{NN}$ with increasing methylation is found to correlate well with the ^{13}C NMR shifts of the naphthalene carbons directly attached to the N centres. However, the lack of correlation of observed and predicted $^{2H}J_{NN}$ with r_{NN} in the aliphatic protonated diamine [**10**H]$^+$, suggests that the participation of the naphthalene ring is not (wholly) responsible for the discrepancy.

Two possible explanations for the increasing $^{2H}J_{NN}$ in the series [**1**–**6**H]$^+$ are i) that the inductive effect of the methyl groups (relative to hydrogen) results in an increased covalency,[56] and thus Fermi-contact, across the cationic N-H-N unit[55] and/or ii) that the significant hydrogen bonding of the N–H units to solvent in the lower members of the homologous series weakens the intramolecular hydrogen bond. The rigidity of the naphthalene skeleton precludes changes in r_{NN} and hence means that the frequently discussed correlation between r_{NN} and $^{2H}J_{NN}$ plays no role in the presently observed highly variable coupling constants. The induction mechanism i) is unlikely as the computed gas-phase coupling constants remain roughly constant with increasing methylation. In contrast, the solvation mechanism ii) is supported by the reduction in computed full spin–spin coupling terms for lower members of the homologous series [**1**–**6**H]$^+$ when microsolvation of the free N–H bonds by discrete DMF is used to reproduce the key aspects of solvent–solute interactions. Further investigation is clearly required and is ongoing in our laboratories. In conclusion, we have demonstrated that solvation of N-H groups, within the confines of the structural restrictions imposed by *intramolecular* N-H-N hydrogen bonding can result in significant deviation of $^{2H}J_{NN}$ between experiment and theory. As such, until $^{2H}J_{NN}/r_{NN}$ values have been determined in a much broader range of species, particularly intermolecular examples (which by their very nature are the hardest to study) caution should be exercised in extracting N-N distances (r_{NN}) from experimental $^{15}N,^{15}N$ coupling constants ($^{2H}J_{NN}$).

Experimental Section

General: The reactions were carried out under nitrogen or hydrogen atmospheres using standard Schlenk techniques. Solvents were dried by passage under nitrogen thorough an Anhydrous Technologies drying train (activated alumina). $Na^{15}NO_3$ (>95 % ^{15}N) was obtained from Amersham International. Flash column chromatography was performed on Merck silica gel 60 or Merck neutral alumina eluting with a constant gravity head of ca. 15 cm solvent. TLC: 0.25 mm, Merck silica gel 60 F254 or neutral alumina F254 visualising at 254 nm or with acidic (H_2SO_4) aq. $KMnO_4$ solution (ca. 2 %). NMR experiments were performed on JEOL GX400 and Delta 400 instruments. Frequency references: ^1H internally referenced to [D_6]DMF = 2.74, 2.91, 8.01 ppm or to CD_2HCN = 1.95 ppm); ^{13}C internally referenced to [D_7]DMF = 30.1, 35.2, 167.7 ppm or to CD_3CN = 118.2, 1.3 ppm; ^{15}N NMR internally referenced to [D_7]DMF = 103.8 ppm or CD_3CN = 239.5 ppm (externally referenced to NH_3 = 0 ppm). Full assignments were aided by 1 and 2D experiments {DEPT, HHCOSY, CH-FGDQFC, CH-FGHMBC} as appropriate. In all cases, ^1J(C,N) is assumed to be negative. Spectral simulation was performed on *g*-NMR software. Mass spectra were recorded on a VG Micromass in electron impact (EI) mode. [**10**H][BF_4] was a gift from Professor Roger W. Alder, University of Bristol.

[$^{15}N_2$]-1,5-dinitronaphthalene and [$^{15}N_2$]-1,8-dinitronaphthalene (**7**). These compounds were prepared by adaptation of a literature method[57] for the preparation of [^{15}N]-1-nitronaphthalene. Naphthalene (1.51 g, 11.77 mmol) and $Na^{15}NO_3$ (2.00 g, 23.26 mmol) were stirred in chloroform (24 mL) at room temperature. A mixture of trifluoroacetic anhydride (17.3 g, 11.64 mL, 82.37 mmol) and trifluoroacetic acid (9.39 g, 6.33 mL, 82.37 mmol) was then added dropwise over 1 h. The resulting yellow suspension was stirred at room temperature for a further 48 h giving a bright yellow homogeneous solution. The reaction was quenched with water (30 mL) and extracted with chloroform (3 × 30 mL). The combined organic phases were dried over $MgSO_4$ and the solvent removed in vacuo to afford the title compounds as an intimate mixture of yellow solids (2.22 g, 86.5 % crude) consisting predominantly of dinitronaphthalenes. Recrystallisation from pyridine three times gave [$^{15}N_2$]-1,5-dinitronaphthalene (330 mg, 12.9 %) as fine yellow needles. M.p. 202–206 °C (from pyridine) (lit. 216 °C[58]); ^1H NMR (400 MHz, $CDCl_3$, 22 °C, $SiMe_4$): δ = 8.29 (ddd, ^3J(H,H) = 7.59, ^4J(H,H) = 1.3, ^3J(N,H) = 2.6 Hz, 2H; C(2)H, C(6)H), 8.25 (dd, ^3J(H,H) = 8.24, ^4J(H,H) = 1.3 Hz, 2H; C(4)H, C(8)H), 7.75 (br dd, ^3J(H,H) = 7.59, ^3J(H,H) = 8.24 Hz, 2H; C(3)H, C(7)H); MS-EI: *m*/*z* (%): 220 (15) [M^+], 173 (81), 142 (22).

The filtrates from the above crystallisations from pyridine were combined and evaporated to give a light brown residue which was recrystallised three times from ethyl acetate to give [$^{15}N_2$]-1,8-dinitronaphthalene ([$^{15}N_2$]-**7**,

805 mg, 31.4%) as pale brown flakes. M.p. 158–160 °C (from ethyl acetate) (lit. 171 °C[58]); ^{1}H NMR (400 MHz, $CDCl_3$, 22 °C, $SiMe_4$): $\delta = 8.80$ (dd, $^3J(H,H) = 7.58$, $^4J(H,H) = 0.8$ Hz, 2H; C(4)H, C(5)H), 8.32 (ddd, $^3J(H,H) = 7.59$, $^4J(H,H) = 0.8$, $^3J(N,H) = 2.2$ Hz, 2H; C(2)H, C(7)H), 7.82 (br dd, $^3J(H,H) = 7.59$, 7.58 Hz, 2H; C(3)H, C(6)H); MS-EI: *m*/*z* (%): 220 (84) [M^+], 173 (7), 142 (14), 126 (75).

[$^{15}N_2$]-1,8-Diaminonaphthalene ([$^{15}N_2$]-1): PtO_2 powder (35 mg, 0.16 mmol) was added to a saturated solution of [$^{15}N_2$]-1,8-dinitronaphthalene (705 mg, 3.204 mmol) in THF (ca. 10.5 mL). The resulting suspension was hydrogenated (1 atm H_2) giving at first a dark brown solution, which after approximately 16 h became lighter as hydrogenation neared completion. The *air sensitive* solution was transferred to a kugelrohr bulb, the solvent removed in vacuo and then brown residue distilled (0.3 mm Hg; oven temperature 120 °C) to give the title compound (446 mg, 87%) as a viscous yellow oil which solidified on standing. M.p. 56–57 °C; (commercial, unlabelled material: m.p. 63–67 °C); ^{1}H NMR (400 MHz, [D$_7$]DMF, 22 °C, [D$_6$]DMF): $\delta = 7.09$ (dd, $^3J(H,H) = 8.06$, 8.06 Hz, 2H; C(3)H, C(6)H), 7.05 (dd, $^3J(H,H) = 8.06$, $^4J(H,H) = 1.71$ Hz, 2H; C(4)H, C(5)H), 6.69 (ddd, $^3J(H,H) = 8.06$, $^4J(H,H) = 1.71$, $^3J(N,H) = 1.96$ Hz, 2H; C(2)H, C(7)H), 5.51 (d, $^1J(N,H) = 78.5$ Hz, 4H; 2 × NH_2); ^{13}C NMR (100.6 MHz {^{1}H}, [D$_7$]DMF, 22 °C, [D$_7$]DMF): $\delta = 147.7$ (X of ABX, C(1), C(8)), 138.4 (s; C(10)), 127.1 (s; C(3)H, C(6)H), 118.9 (s; C(4)H, C(5)H), 117.7 (t, $^2J(C,N) = 2.02$ Hz; C(9)), 111.4 (s; C(2)H, C(7)H); ^{15}N NMR (40.6 MHz, [D$_7$]DMF, 22 °C, [D$_7$]DMF): $\delta = 62.7$ (t, $^1J(N,H) = 78.5$ Hz, 2N; NH_2); MS-EI: *m*/*z* (%): 160 (100) [M^++H], 145 (3), 131 (28).

[$^{15}N_2$]-*N*-Methyl-1,8-diaminonaphthalene, [$^{15}N_2$]-*N*,*N*-dimethyl-1,8-diaminonaphthalene, [$^{15}N_2$]-*N*,*N*′-dimethyl-1,8-diaminonaphthalene and [$^{15}N_2$]-*N*,*N*,*N*′-trimethyl-1,8-diaminonaphthalene: Sodium hydride 60% dispersion (80 mg, 2.0 mmol) was added to a stirred solution of [$^{15}N_2$]-1,8-diaminonaphthalene (315 mg, 1.97 mmol in THF (4.8 mL). After effervescence had ceased, the brown solution was stirred at room temperature for 15 min and then methyl iodide (280 mg, 0.120 mL, 1.97 mmol) added dropwise, resulting in a pale green suspension. After 15 minutes, a further portion of sodium hydride 60% dispersion (80 mg, 2.0 mmol) and methyl iodide (280 mg, 0.120 mL, 1.97 mmol) was added, resulting in an off-white suspension. After stirring for a further 3 h, the reaction mixture was cautiously quenched with water (5 mL) and then extracted with ethyl acetate (3 × 5 mL). The combined organic phases were dried ($MgSO_4$) and the solvent removed in vacuo to give a dark brown tar. This was purified by column chromatography on neutral alumina using column of dimensions 12.5 cm (length) and 4.3 cm (diameter). Elution with a gradient from 1 to 100% ethyl acetate in hexane gave: [$^{15}N_2$]-**2**, [$^{15}N_2$]-**3**, [$^{15}N_2$]-**4** and [$^{15}N_2$]-**5**.

[$^{15}N_2$]-*N*-methyl-1,8-diaminonaphthalene ([$^{15}N_2$]-2): (90 mg, 26.2%); R_f (90% hexane/10% EtOAc; neutral alumina, 0.24); ^{1}H NMR (400 MHz, [D$_7$]DMF, 22 °C, [D$_6$]DMF): $\delta = 7.28$ (d, $^3J(H,H) = 8.79$ Hz, 1H; C(5)H), 7.20 (dd, $^3J(H,H) = 7.57$, 8.07 Hz, 1H; C(3)H), 7.14 (dd, $^3J(H,H) = 6.60$, 8.79 Hz 1H; C(6)H), 7.04 (dd, $^3J(H,H) = 8.07$, $^4J(H,H) = 1.22$ Hz, 1H; C(4)H), 5.70 (very broad signal, 3H; NH and NH_2), 6.65 (d, $^3J(H,H) = 6.60$ Hz, 1H; C(7)H), 6.42 (dd, $^3J(H,H) = 7.57$, $^4J(H,H) = 1.22$ Hz, 1H; C(2)H), 2.84 (s, 3H; Me); ^{13}C NMR(100.6 MHz {^{1}H}, [D$_7$]DMF, 22 °C, [D$_7$]DMF): $\delta = 149.5$ (d, $^1J(C,N) = -11.53$ Hz; C(1)), 146.9 (d, $^1J(C,N) = -8.84$ Hz; C(8)), 135.0 ($^3J(C,N) = 2.7$, 2.7 Hz; (10)), 129.9 (s; C(4)), 119.8 (s; C(5)), 117.9 (s; C(3)), 117.8 (dd, $^2J(C,N) = 2.1$, 2.1 Hz; C(9)), 115.3 (s; C(6)), 113.2 (d, $^2J(C,N = 0.77$ Hz; C(2)), 104.9 (s; C(7)), 31.9, (d, $^1J(C,N) = -9.22$ Hz; Me); ^{15}N NMR (40.6 MHz {^{1}H}, [D$_7$]DMF, 22 °C, [D$_7$]DMF): $\delta = 61.7$ (d, $^{2H}J(N,N) = 3.25$ Hz, 1N; NH_2), 59.5 (d, $^{2H}J(N,N) = 3.25$ Hz, 1N; HNMe).

[$^{15}N_2$]-*N*,*N*′-Dimethyl-1,8-diaminonaphthalene ([$^{15}N_2$]-3): (14 mg, 3.8%); R_f (90% hexane/10% EtOAc; neutral alumina, 0.51); ^{1}H NMR (400 MHz, [D$_7$]DMF, 22 °C, [D$_6$]DMF): $\delta = 7.24$ (dd, $^3J(H,H) = 7.60$, 7.60, 2H; C(3), C(6)H), 7.14 (d, $^3J(H,H) = 7.60$, 2H; C(4), C(5)H), 6.55 (d, $^3J(H,H) = 7.60$, 2H; C(2)H, C(7)H), 6.19 (dq, $^3J(H,H) = 5.25$, $^1J(NH) = 83.35$ Hz, 2H; 2 × NH), 2.76 (d, $^3J(H,H) = 5.25$ Hz, 6H; 2 × Me); ^{13}C NMR (100.6 MHz {^{1}H}, [D$_7$]DMF, 22 °C, [D$_7$]DMF): $\delta = 149.2$ (X of ABX; C(1), C(8)), 137.8 (t, $^2J(C,N) = 1.10$ Hz; C(10)),127.3 (s; C(3), C(6)), 119.0 (s; C(4), C(5)), 117.8 (t, $^2J(C,N) = 2.21$ Hz; C(9)), 102.0 (d, $^2J(C,N) = 1.6$ Hz; C(2), C(7)), 32.8 (X of ABX; 2 × Me); ^{15}N NMR (40.6 MHz, [D$_7$]DMF, 22 °C, [D$_7$]DMF): $\delta = 37.8$ (d, $^1J(N,H) = 83.35$ Hz, 2N; HNMe).

[$^{15}N_2$]-*N*,*N*-Dimethyl-1,8-diaminonaphthalene ([$^{15}N_2$]-4): (53 mg, 14.2%); R_f (90% hexane/10% EtOAc; neutral alumina, 0.44); ^{1}H NMR(400 MHz, [D$_7$]DMF, 22 °C, [D$_6$]DMF: $\delta = 7.48$ (dd, $^3J(H,H) = 8.07$, $^4J(H,H) = 1.22$, 1H; C(4)H), 7.30 (dd, $^3J(H,H) = 8.07$, 8.07, 1H; C(3)H), 7.16 (dd, $^3J(H,H) = 7.57$, 7.57, 1H; C(6)H), 7.16 (dd, $^3J(H,H) = 7.57$, $^4J(H,H) = 1.47$ Hz, 1H; C(5)H), 7.02 (dd, $^3J(H,H) = 8.07$, $^4J(H,H) = 1.22$ Hz, 1H; C(2)H), 6.93 (very broad singlet, 2H; NH_2), 6.66 (ddd, $^3J(H,H) = 7.57$, $^4J(H,H) = 1.47$, $^3J(N,H) = 2.44$ Hz, 1H; C(7)H), 2.74 (s, 6H; Me); ^{13}C NMR (100.6 MHz {^{1}H}, [D$_7$]DMF, 22 °C, [D$_7$]DMF): $\delta = 153.5$ (d, $^1J(C,N) = -7.00$ Hz; C(1)), 148.0 (d, $^1J(C,N) = -12.30$ Hz; C(8)), 138.4 (s; C(10)), 127.8 (s; C(3)H), 126.3 (s; C(5)H), 125.9 (s; C(4)H), 119.1 (d, $^2J(H,H) = 4.70$ Hz; C(9)), 116.2 (s; C(6)H), 115.4 (s; C(2)H), 109.6 (d, $^2J(C,N) = 2.30$ Hz; C(7)H), 46.6 (d, $^1J(C,N) = -5.38$ Hz; NMe_2); ^{15}N NMR (40.6 MHz {^{1}H}, [D$_7$]DMF, 22 °C, [D$_7$]DMF): $\delta = 62.5$ (d, $^{2H}J(N,N) = 3.28$ Hz, 1N; NH_2), 35.8 (d, $^{2H}J(N,N) = 3.28$ Hz, 1N; NMe_2).

[$^{15}N_2$]-*N*,*N*,*N*′-Trimethyl-1,8-diaminonaphthalene ([$^{15}N_2$]-5): (171 mg, 43.1%); R_f (90% hexane/10% EtOAc; neutral alumina, 0.71); ^{1}H NMR (400 MHz, [D$_7$]DMF, 22 °C, [D$_6$]DMF): $\delta = 8.99$ (d, $^1J(N,H) = 88.54$ Hz; 1H, NH), 7.52 (dd, $^3J(H,H) = 8.06$,$^4J(H,H) = 1.22$ Hz; 1H, C(4)H), 7.33 (dd, $^3J(H,H) = 7.58$, 7.58 Hz 1H; C(6)H), 7.27 (dd, $^3J(H,H) = 8.06$, 7.43 Hz, 1H; C(3)H), 7.22 (dd, $^3J(H,H) = 7.58$, $^4J(H,H) = 1.22$ Hz, 1H; C(5)H),7.02 (dd, $^3J(H,H) = 7.43$, $^4J(H,H) = 1.22$ Hz, 1H; C(2)H), 6.40 (dd, $^3J(H,H) = 7.58$, $^3J(H,H) = 1.22$ Hz, 1H; C(7)H), 2.94 (s, 3H, HNMe), 2.72 (s, 6H, NMe_2); ^{13}C NMR (100.6 MHz {^{1}H}, [D$_7$]DMF, 22 °C, [D$_7$]DMF): $\delta = 153.3$ (d, $^1J(C,N) = -6.92$ Hz; C(1)), 149.2 (d, $^1J(C,N) = -13.46$ Hz; C(8)), 138.1 (dd, $^3J(C,N) = 1.16$, 0.77 Hz; C(10)), 128.1 (d, $^3J(C,N) = 1.15$ Hz; C(3)H), 126.5 (d, $^2J(C,N) = 0.76$ Hz; C(2)H), 126.2 (s; C(4)H), 119.1 (dd, $^2J(C,N) = 3.84$, 0.76 Hz; C(9)), 116.1 (s; C(6)H), 115.6 (s; C(5)H), 103.25 (d, $^2J(C,N) = 1.54$ Hz; C(7)H), MeNH peak obscured by D_n-DMF signal, 46.5 (d, $^1J(C,N) = -5.38$ Hz; NMe_2); ^{15}N NMR (40.6 MHz, [D$_7$]DMF, 22 °C, [D$_7$]DMF): $\delta = 58.6$ (dd, $^1J(N,H) = 88.54$, $^{2H}J(N,N) = 3.71$ Hz, 1N; HNMe), 35.1 (d, $^{2H}J(N,N) = 3.71$ Hz, 1N; NMe_2).

[$^{15}N_2$]-*N*,*N*,*N*′,*N*′-Tetramethyl-1,8-diaminonaphthalene ([$^{15}N_2$]-6): A solution of the HI salt of [$^{15}N_2$]-*N*,*N*,*N*′,*N*′-tetramethyl-1,8-diaminonaphthalene (40 mg, 0.116 mmol) in CH_2Cl_2 (1 mL) was washed with 3 M NaOH solution (3 × 2 mL), the organic phase was separated, dried ($MgSO_4$) and the solvent removed in vacuo to give the title compound as a pale orange viscous oil (23 mg, 91%). ^{1}H NMR (400 MHz, [D$_7$]DMF, 22 °C, [D$_6$]DMF): $\delta = 7.40$ (d, $^3J(H,H) = 7.33$ Hz, 2H; C(4), C(5)H), 7.32 (dd, $^3J(H,H) = 7.33$, 7.33 Hz, 2H; C(3), C(6)H), 6.99 (d, $^3J(H,H) = 7.33$ Hz, 2H; C(2), C(7)H), 2.78 (s, 12H; 4 × Me); ^{13}C NMR (100.6 MHz {^{1}H}, [D$_7$]DMF, 22 °C, [D$_7$]DMF): $\delta = 151.7$ (d, $^1J(C,N) = -10.76$ Hz; C(1), C(8)), 139.0 (s; C(10)), 126.6 (s; C(4)H, C(5)H), 122.7 (s; C(3)H, C(6)H), 121.5 (t, $^2J(H,H) = 3.83$ Hz; C(9)), 113.9 (s; C(2)H, C(7)H), 45.0 (d, $^1J(H,H) = -8.00$ Hz; 4 × Me); ^{15}N NMR (40.6 MHz {^{1}H}, [D$_7$]DMF, 22 °C, [D$_7$]DMF): $\delta = 46.0$ (s; NMe_2).

General procedure for mono-protonation of the free-base forms of amines 1–5 with ethereal HI: Conc. HCl (0.67 mL, 8 mmol) was added to a saturated solution of sodium iodide (1.509 g, 10 mmol) in acetonitrile (ca. 5 mL) immediately resulting in a white precipitate. Diethyl ether was then added until precipitation of inorganic salts was complete and the resulting yellow solution used immediately. The amine, as solution in ether was treated dropwise with the ethereal HI solution until precipitation had ceased, the supernatant liquid was removed by pipette and then the solid dried under a stream of nitrogen to give the hydrogen iodide salt as a yellow powder.

HI salt of [$^{15}N_2$]-1,8-diaminonaphthalene (1): Prepared using the general procedure outlined above; m.p. 168–172 °C (decomp); ^{1}H NMR (400 MHz, [D$_7$]DMF, 22 °C, [D$_6$]DMF): $\delta = 9.36$ (br s, 5H; NH_2 and NH_3^+), 7.81 (dd, $^3J(H,H) = 7.07$, $^4J(H,H) = 1.47$ Hz, 2H; C(4), C(5)H), 7.52 (dd, $^3J(H,H) = 7.07$, 7.07 Hz 2H; C(3)H, C(6)H), 7.48 (ddd, $^3J(H,H) = 7.07$, $^4J(H,H) = 1.47$, $^3J(N,H) = 2.22$ Hz, 2H; C(2)H, C(7)H); ^{13}C NMR (100.6 MHz {^{1}H}, [D$_7$]DMF, 22 °C, [D$_7$]DMF): $\delta = 135.9$ (s; C(10)), 133.2 (X of ABX; C(1), C(8)), 133.1 (s; C(4)H, C(5)H), 129.7 (d, $^3J(C,N) = 2.31$ Hz; C(3)H, C(6)H), 117.6 (broad singlet; C(9)), 109.5 (d, $^2J(C,N) = 2.69$ Hz; C(2)H, C(7)H); ^{15}N NMR(40.6 MHz {^{1}H}, [D$_7$]DMF, 22 °C, [D$_7$]DMF): $\delta = 62.1$ (s; NH_2 and NH_3^+).

HI salt of [$^{15}N_2$]-*N*-methyl-1,8-diaminonaphthalene (2): Prepared using the general procedure outlined above; m.p. 182–185 °C (decomp); ^{1}H NMR (400 MHz, [D$_7$]DMF, 22 °C, [D$_6$]DMF): $\delta = 8.85$ (very broad singlet, 5H; $H_2N\cdots H\cdots NH_2^+$), 7.96–7.92 (*m*, 1H; C(4)H), 7.86 (dd, $^3J(H,H) = 8.3$, $^4J(H,H) = 1.22$ Hz, 1H; C(5)H), 7.61 (dd, $^3J(H,H) = 7.57$, 7.57 Hz, 1H;

C(3)H), 7.60–7.55 (*m*, 2H; C(7)H, C(6)H), 7.51 (ddd, ^{3}J(H,H) = 7.57, ^{4}J(H,H) = 1.22, ^{3}J(N,H) = 1.95 Hz 1H; C(2)H), 3.05 (s, 3H; Me); ^{13}C NMR (100.6 MHz {^{1}H}, [D$_7$]DMF, 22 °C, [D$_7$]DMF): δ = 135.7 (s; C(10)),135.1 (d, ^{1}J(C,N) = −13.07 Hz; C(8)), 132.5 (d, ^{1}J(C,N) = −12.68 Hz; C(1)), 129.7 (d, ^{2}J(C,N) = 2.31 Hz; C(7)H), 129.6 (d, ^{2}J(C,N) = 1.92 Hz; C(2)H), 124.8 (s; C(5)), 124.1 (s; C(4)), 122.3 (brs; C(9)), 109.9 (d ^{3}J(C,N) = 1.93 Hz; C(6)H), 108.6 (s; C(3)H), 39.5 (d, ^{1}J(C,N) = −10.00 Hz; Me); ^{15}N NMR (40.6 MHz {^{1}H}, [D$_7$]DMF, 22 °C, [D$_7$]DMF): δ = 48.4 (d, ^{2H}J(N,N) = 2.60 Hz, 1H; NH_3^+), 47.1 (d, ^{2H}J(N,N) = 2.60 Hz, 1N; MeNH).

HI salt of [^{15}N$_2$]-*N,N′*-dimethyl-1,8-diaminonaphthalene (3): Prepared using the general procedure outlined above; m.p. 170–173 °C (decomp); ^{1}H NMR (400 MHz, [D$_7$]DMF, 22 °C, [D$_6$]DMF): δ = 8.43 (br d ^{1}J(N,H) = 92.0 Hz, 2H; NH_2^+), 7.68 (d, ^{3}J(H,H) = 8.30 Hz, 2H; C(4)H, C(5(H), 7.48 (dd, ^{3}J(H,H) = 7.57, 8.30 Hz, 2H; C(3)H, C(6)H), 7.14 (dd, ^{3}J(H,H) = 7.57, ^{3}J(N,H) = 1.95 Hz, 2H; C(2)H, C(7)H), 3.69 (d, ^{3}J(N,H) = 1.22 Hz, 6H; 2 × Me); ^{13}C NMR (100.6 MHz {^{1}H}, [D$_7$]DMF, 22 °C, [D$_7$]DMF): δ = 136.6 (s, C(10)), 133.7 (X of ABX; C(1), C(8)), 124.5 (s; C(4), C(5)), 123.5 (s; C(3), C(6)), 122.4 (t, ^{2}J(C,N) = 0.90 Hz; C(9)), 108.4 (d, ^{3}J(C,N) = 1.40 Hz; C(2), C(7)), 38.8 (X of ABX; 2 × Me); ^{15}N NMR (40.6 MHz {^{1}H}, [D$_7$]DMF, 22 °C, [D$_7$]DMF): δ = 51.54 (s; 2 × Me(H)N-H).

HI salt of [^{15}N$_2$]-*N,N*-dimethyl-1,8-diaminonaphthalene (4): Prepared using the general procedure outlined above; m.p. 126–130 °C (decomp); ^{1}H NMR (400 MHz, [D$_7$]DMF, 22 °C, [D$_6$]DMF): δ = 8.11 (dd, ^{3}J(H,H) = 7.57, ^{4}J(H,H) = 1.47 Hz, 1H; C(5)H), 8.03 (dd, ^{3}J(H,H) = 8.56, ^{4}J(H,H) = 1.23 Hz, 1H; C(4)H), 7.92 (ddd, ^{3}J(H,H) = 7,.57, ^{4}J(H,H) = 1.47, ^{3}J(N,H) = 1.72 Hz, 1H; C(7)H), 7.71 (dd, ^{3}J(H,H) = 8.56, ^{4}J(H,H) = 1.23 Hz, 1H; C(2)H), 7.71 (dd, ^{3}J(H,H) = 8.56, 8.56, 1H; C(3)H), 7.68 (dd, ^{3}J(H,H) = 7.57, 7.57, 1H; C(6)H), 4.21 (very broad singlet, 3H; NH_3^+), 2.98 (s, 6H; NMe_2); ^{13}C NMR (100.6 MHz {^{1}H}, [D$_7$]DMF, 22 °C, [D$_7$]DMF): δ = 149.6 (d, ^{1}J(C,N) = −6.92 Hz; C(1)), 136.8 (s; C(10)), 130.5 (d, ^{1}J(C,N) = −8.07 Hz; C(8)), 129.7 (s; C(4)H), 128.2 (s, (C(5)H), 128.1 (s; C(3)H), 127.0 (d, ^{2}J(C,N) = 1.54 Hz; C(2)H), 124.8 (s; C(6)H), 122.9 (d, ^{2}J(C,N) = 3.46 Hz; C(9)),122.2 (s; C(7)H), 46.4 (d, ^{1}J(C,N) = −4.99 Hz; Me); ^{15}N NMR (40.6 MHz {^{1}H}, [D$_7$]DMF, 22 °C, [D$_7$]DMF): δ = 44.7 (d, ^{2H}J(N,N) = 4.46 Hz, 1N; NH_3^+), 32.9 (d, ^{2H}J(N,N) = 4.46 Hz, 1N; NMe_2).

HI salt of [^{15}N$_2$]-*N,N,N′*-trimethyl-1,8-diaminonaphthalene (5): Prepared using the general procedure outlined above; m.p. 193–195 °C; ^{1}H NMR (400 MHz, [D$_7$]DMF, 22 °C, [D$_6$]DMF): δ = 12.90 (very broad singlet, 2H; NH_2^+), 8.07 (dd, ^{3}J(H,H) = 7.57, ^{4}J(H,H) = 1.46 Hz, 1H; C(4)H), 8.05 (d, ^{3}J(H,H) = 8.06 Hz, 1H; C(5)H), 7.97 (dd, ^{3}J(H,H) = 7.57, ^{4}J(H,H) = 1.46, 1H; C(2)H), 7.82 (brd, ^{3}J(H,H) = 8.06 Hz, 1H; C(7)H), 7.72 (dd, ^{3}J(H,H) = 7.57, 7.57 Hz, 1H; C(3)H), 7.71 (dd, ^{3}J(H,H) = 8.06, 8.06 Hz, 1H; C(6)H), 3.30 (s, 3H; MeN), 3.03 (s, 6H; NMe_2); ^{13}C NMR (100.6 MHz {^{1}H}, [D$_7$]DMF, 22 °C, [D$_7$]DMF): δ = 149.4 (d, ^{1}J(C,N) = −6.92 Hz; C(1)), 138.8 (d, ^{1}J(C,N) = −8.84 Hz; C(8)), 136.8 (s; C(10)H), (s; C(10)), 129.0 (s; C(3)H), 128.7 (s; C(6)H), 129.2 (s; C(5)H), 127.5 (d, ^{2}J(C,N) = 1.15 Hz; C(7)H), 122.5 (s; C(2)H), 122.3 (s; C(4)H), 121.7 (d, ^{2}J(C,N) = 3.46 Hz; (C(9)), 46.7 (d, ^{1}J(C,N) = −4.99 Hz; NMe_2), 37.9 (d, ^{1}J(C,N) = −5.77 Hz; $MeNH_2^+$); ^{15}N NMR (40.6 MHz {^{1}H}, [D$_7$]DMF, 22 °C, [D$_7$]DMF): δ = 41.7 (d, ^{2H}J(N,N) = 6.68 Hz, 1N; $MeNH_2^+$), 32.8 (d, ^{2H}J(N,N) = 6.68 Hz, 1N; NMe_2).

HI salt of [^{15}N$_2$]-*N,N,N′,N′*-tetramethyl-1,8-diaminonaphthalene (6): [^{15}N$_2$]-*N,N,N′*-Trimethyl-1,8-diaminonaphthalene (100 mg, 0.494 mmol) was dissolved in excess methyl iodide (2.280 g, 1 mL, 16.063 mmol) to give a pale yellow solution which was left at room temperature for 72 h. The excess methyl iodide was decanted from the pale yellow needles which had formed and they were washed with a further portion of methyl iodide (0.5 mL) and then the residual solvent removed in vacuo to afford the HI salt of the title compound as a yellow powder (131 mg, 77%). M.p. 248–250 °C (from MeI); ^{1}H NMR (400 MHz, [D$_7$]DMF, 22 °C, [D$_6$]DMF): δ = 18.68 (triple tridecet, ^{1}J(N,H) = 30.53, ^{3}J(H,H) = 2.44 Hz, 1H; NH$^+$), 8.22 (dd, ^{3}J(H,H) = 7.57, ^{4}J(H,H) = 0.98 Hz, 2H; C(4), C(5)H), 8.19 (dd, ^{3}J(H,H) = 8.31, ^{4}J(H,H) = 0.98 Hz, 2H; C(2), C(7)H), 7.80 (dd, ^{3}J(H,H) = 8.31, 7.57 Hz, 2H; C(3), C(6)H), 3.34 (d, ^{3}J(H,H) = 2.44 Hz, 12H; Me); ^{13}C NMR (100.6 MHz {^{1}H}, [D$_7$]DMF, 22 °C, [D$_7$]DMF): δ = 146.1 (X of ABX; C(1), C(8)), 136.4 (s; C(10)), 130.1 (s; C(4), C(5))128.1 (s; C(3), C(6)), 123.1 (s; C(2), C(7)), 120.5 (t, ^{2}J(C,N) = 2.21 Hz; C(9)), 46.9 (X of ABX; 4 × Me); ^{15}N NMR (40.6 MHz, [D$_7$]DMF, 22 °C, [D$_7$]DMF): δ = 35.32 (d, ^{1}J(N,H) = 30.53 Hz; H···NMe_2).

Trifluoromethanesulphonic acid salt of [^{15}N$_2$]-*N,N,N′,N′*-tetramethyl-1,8-diaminonaphthalene (6): In an NMR tube, trifluoromethanesulphonic acid (11 mg, 11 μL, 0.07 mmol) was added to a solution of [^{15}N$_2$]-*N,N,N′,N′*-tetramethyl-1,8-diaminonaphthalene (15 mg, 0.07 mmol) in [D$_7$]DMF (1 g) to give a pale yellow solution. The ^{1}H, ^{13}C, and ^{15}N NMR spectra were recorded immediately. ^{1}H NMR (400 MHz, [D$_7$]DMF, 22 °C, [D$_6$]DMF): δ = 18.66 (triple tridecet, ^{1}J(N,H) = 34.9, ^{3}J(H,H) = 2.68 Hz, 1H, NH$^+$), 8.20 (dd, ^{3}J(H,H) = 7.33, ^{4}J(H,H) = 0.98 Hz, 2H; C(4), C(5)H), 8.19 (dd, ^{3}J(H,H) = 7.33, ^{4}J(H,H) = 0.98 Hz, 2H; C(2), C(7)H), 7.79 (dd, ^{3}J(H,H) = 7.33, 7.33 Hz, 2H; C(3), C(6)H), 3.32 (d, ^{3}J(H,H) = 2.68 Hz, 12H; Me); ^{13}C NMR (100.6 MHz {^{1}H}, [D$_7$]DMF, 22 °C, [D$_7$]DMF): δ = 146.0 (X of ABX; C(1), C(8)), 136.3 (s; C(10)), 130.1 (s; C(4), C(5)), 128.1 (s; C(3), C(6)), 122.9 (s; C(2), C(7)), 120.5 (t, ^{2}J(C,N) = 1.92 Hz; C(9)), 46.7 (X of ABX; 2 × NMe_2); ^{15}N NMR (40.6 MHz, [D$_7$]DMF, 22 °C, [D$_7$]DMF): δ = 34.9 (d, ^{1}J(N,H) = 30.62 Hz; 2 × NMe_2).

Tetrafluoroboric acid salt of [^{15}N$_2$]-1,6-dimethyl-1,6-diazacyclodecane (10): ^{1}H NMR (400 MHz, [D$_7$]DMF, 22 °C, [D$_6$]DMF): δ = 19.51 (tm, ^{1}J(N,H) = 28.81 Hz, 1H; NH), 2.89–2.79 (m, 4H; NCH*H*), 2.61 (d, ^{3}J(H,H) = 2.50 Hz, 6H; Me), 2.69–2.59 (m, 4H; NCH_2), 1.83 (brs, 8H; NCH_2CHH); ^{13}C NMR (100.6 MHz {^{1}H}, [D$_7$]DMF, 22 °C, [D$_7$]DMF): δ = 54.6 (s; 4 × NCH_2), 41.1 (X of ABX; 2 × Me), 25.7 (s; 4 × NCH_2CH_2); ^{15}N NMR (40.6 MHz, [D$_7$]DMF, 22 °C, [D$_7$]DMF): δ = 43.4 (d, ^{1}J(NH) = 28.81 Hz, 1H; 2 × CH_2N(H)Me). ^{1}H NMR (400 MHz, CD_3CN, 22 °C, CD_3CN) δ = 19.35 (tm, ^{1}J(N,H) = 30.44 Hz, 1H; NH), 2.76–2.65 (m, 4H; NC*H*H), 2.56 (d, ^{3}J(H,H) = 2.69 Hz, 6H; 2 × Me), 2.56–2.47 (m, 4H; NCH*H*, 1.82 (brs, 8H; NCH_2CH_2); ^{13}C NMR (100.6 MHz {^{1}H}, CD_3CN, 22 °C, CD_3CN): δ = 55.7 (s; 4 × NCH_2), 42.2 (X of ABX; 2 × Me), 26.8 (s; 4 × NCH_2CH_2); ^{15}N NMR (40.6 MHz, CD_3CN, 22 °C, CD_3CN): δ = 42.9 (d, ^{1}J(N,H) = 30.44 Hz; 2 × N).

Determination of $J_{AA'}$ and J_{AB} in the X-part of AA′X and ABX spectra: The ^{13}C{^{1}H} NMR spectra of the time-average symmetrical, doubly ^{15}N-labelled, species ([^{15}N$_2$]-**1**, [^{15}N$_2$]-**3**, [^{15}N$_2$]-**6** and [^{15}N$_2$]-[**1**H][I], [^{15}N$_2$]-[**6**H][I]) are of the ABX type (^{15}N = A,B; ^{13}C = X), since an isotope effect renders the two ^{15}N nuclei chemically non-equivalent. Since this shift is small, the observed spectra look similar to the AA′X spectra which would be observed if there were no isotope shift. The X part of an AA′X spectrum consists of six transitions, two of which occur at δ_X. The remaining four transitions form two pairs, each symmetrically placed about δ_X, one with a separation equal to N (J_{AX}+$J_{A'X}$), the other with a separation equal to $\sqrt{(L^2+4J^2)}$, where L = J_{AX} − $J_{A'X}$, and J = $J_{AA'}$). Clearly it is impossible to determine the three coupling constants from these two separations alone. Further information is however available from the line intensities. Whereas the N doublet has 50% of the total intensity, the distribution of the remaining 50% intensity between the central line and the $\sqrt{(L^2\sqrt{4J^2})}$ doublet varies, depending on the ratio of L to J. Thus if J ≫ L, the central line has 50% of the total intensity, the $\sqrt{(L^2+4J^2)}$ doublet has zero intensity, and only a triplet is observed. Neither J nor L can be determined. If J ≪ L, the central line has zero intensity, the remaining doublet has 50% of the total intensity, and a doublet of doublets is observed. If J is then assumed to be zero (not necessarily justified if L is large), L can be determined, so J_{AX} and $J_{A'X}$ can be determined. However, since in this case N and L cannot be distinguished, it is impossible to determine the relative signs of J_{AX} and $J_{A'X}$. In intermediate cases (J ≈ L), five lines are observed, and the relative intensities of the central line and the $\sqrt{(L^2+4J^2)}$ doublet allow a complete analysis. The accuracy with which J (and therefore L) can be determined will however vary as J approaches the two extreme conditions described above. The approach we have used is to perform full band-shape analysis to simulate the spectrum with respect to both frequency and intensity. If the isotope shift between the two A nuclei is significant (for ^{12}C/^{13}C this usually implies that one of the ^{13}C nuclei is directly bonded to the X nucleus) the system must be treated as an ABX system, with the introduction of a fourth parameter, ΔAB. To a first approximation, the only effect of the isotope shift is to split the central line. This splitting depends on ΔAB, but not in a linear fashion. Adding the chemical shift to the simulations is relatively trivial; it can be quickly determined since the separation of the two central lines depends largely on the shift ΔAB. By performing full band shape analysis of the X part, as we have done, there is no necessity to measure the spectra at different field strengths. The approach used in earlier work[18] was to measure the spectra at three different field strengths, and use the (non-linear) variation of the central splitting to determine the parameters. This approach is of course not

Table 3. $^{13}C\{^1H\}$ NMR parameters used in simulation of X part of ABX spectra of $[^{15}N_2]$-**1**, $[^{15}N_2]$-**3**, $[^{15}N_2]$-**6**, $[^{15}N_2]$-[**1**H][I], $[^{15}N_2]$-[**6**H][I], $[^{15}N_2]$-[**6**H][OTf], $[^{15}N_2]$-[**6**H][ClO_4] and $[^{15}N_2]$-[**10**H][BF_4].[a]

Species	Solvent	J_{AB}[a] [Hz]	J_{AX}[a] [Hz]	J_{BX}[a] [Hz]	$[\tilde{\nu}_A\text{-}\tilde{\nu}_B]$[a] [ppb]	$\omega_{0.5}$[a] [Hz]
$[^{15}N_2]$-**1**	[D_7]DMF	2.88 (0.3)	– 9.43 (0.3)	0.17 (0.15)	20 (5)	0.5 (0.25)
$[^{15}N_2]$-[**1**H][I]	[D_7]DMF	1.50 (0.5)	– 12.50 (0.2)	1.5 (0.20)	40 (40)	0.80 (0.15)
$[^{15}N_2]$-**3**	[D_7]DMF	3.28 (0.3)	– 10.48 (0.2)	0.66 (0.15)	17 (5)	0.4 (0.15)
$[^{15}N_2]$-[**3**H][I][b]	[D_7]DMF	2.5 (0.5)[b]	– 12.6 (0.2)[b]	0.75 (0.2)[b]	17 (5)[b]	0.80 (0.15)[b]
$[^{15}N_2]$-**6**	[D_7]DMF	0 (0.5)	– 10.76 (0.2)	0.77 (0.5)	–	0.4 (0.1)
$[^{15}N_2]$-**6**[c]	CD_3CN	0 (0.5)	– 11.1	0.8 (0.5)	–	–[d]
$[^{15}N_2]$-[**6**H][I]	[D_7]DMF	8.46 (0.2)	– 7.62 (0.2)	1.16 (0.20)	25 (5)	0.4 (0.1)
$[^{15}N_2]$-[**6**H][OTf]	[D_7]DMF	8.80 (0.3)	– 6.90 (0.3)	0.60 (0.30)	31 (5)	0.45 (0.15)
$[^{15}N_2]$-[**6**H][ClO_4][c]	CD_3CN	8.7 (0.5)	– 7.4 (0.5)	1.0 (0.5)	26 (8)[e]	–[d]
$[^{15}N_2]$-[**10**H][BF_4]	[D_7]DMF	10.56 (0.5)	– 5.47 (0.4)	0.42 (0.5)	34 (30)	1.95 (0.2)
$[^{15}N_2]$-[**10**H][BF_4]	CD_3CN	10.60 (0.5)	– 6.22 (0.4)	1.05 (0.5)	23 (20)	1.50 (0.2)

[a] For full details of simulation and parameters, see discussion in Experimental Section; C(1,8) are source of ^{13}C signals for $[^{15}N_2]$-**1**, $[^{15}N_2]$-**3**, $[^{15}N_2]$-**6**, $[^{15}N_2]$-[**1**H][I], $[^{15}N_2]$-[**6**H][I], $[^{15}N_2]$-[**6**H][OTf and $[^{15}N_2]$-[**6**H][ClO_4]. Methyl groups are source of ^{13}C signals for $[^{15}N_2]$-[**10**H][BF_4]. [b] Quality of spectrum rather poor (see ref. [27]), consequently data not as reliable as other entries. [c] Data taken from ref. [18]. [d] Line widths vary with field (0.5 to 1.2 Hz) in original publication (ref. [18]). [e] Note that in ref. [18] the isotope shift is incorrectly given as 2.6(8) ppb.

always available, and the accuracy of using line separations alone must be questioned, since the critical central splitting, even on a 17.7 T spectrometer, is no more than 2–3 Hz.

Simulation of $^{13}C\{^1H\}$ sub-spectra: The real FID was transformed into *g*-SPG format by conversion first to JEOL GX file format using JEOL delta software, then subsequently into *g*-NMR spectral format using commercially available *g*-CVT software. The unweighted 65 536 point spectrum was phased and calibrated using commercially available *g*-SPG software. Spectral analysis of the X part of the 3 spin ABX (^{15}N,^{15}N,$^{13}C(1,8)$) system was conducted by iterative automated simulation with commercially available *g*-NMR software such that a best fit was obtained on the basis of both frequency and intensity (full bandshape analysis). Of the seven required parameters [J_{AB} (= $J_{NN'}$); J_{AX} (= J_{CN}); J_{BX} (= $J_{CN'}$); $\tilde{\nu}_A$; $\tilde{\nu}_B$ ($\tilde{\nu}_A - \tilde{\nu}_B = \Delta\delta$ ^{15}N, the isotope shift); $\tilde{\nu}_X$ and the natural line-width $\omega_{0.5}$], the following were variables: {J_{AB}, J_{AX}, J_{BX}, $\tilde{\nu}_A$} and the following were fixed {$\tilde{\nu}_B$, $\tilde{\nu}_X$, $\omega_{0.5}$}. The fixed parameters were obtained from the real ^{15}N and ^{13}C spectra. We note that the simulation did not take into account the small variations in line widths within sub-spectra (i.e., a single value of $\omega_{0.5}$ was applied to the system). However, these variations are usually neglible.[46b] With the best-fit in hand, the tolerance of the fit to each of the parameters was approximated by locking six of the seven "best fit parameters" and, in turn, allowing freedom in a seventh parameter until the fit became noticeably poorer. The data for the simulations are collected in Table 3.

Computational methods: The geometry of all species was fully optimised using the Jaguar 4.1 code[59] at the standard B3LYP level of theory, with the flexible 6-311G(d,p) basis set on all atoms. For the bare diamines and protonated species, all possible conformers and/or tautomers were optimised separately, and the reported data refers to the lowest-lying amongst the tautomers. Transition states for proton transfer for the non- and tetra-methylated species were optimised by restricting the geometry to C_{2v} symmetry. The geometry of the cationic species was re-optimised using a polarisable continuum model "solvent", as implemented in Jaguar, using solvent parameters ($\varepsilon = 38.3$, probe radius = 2.485 Å) suitable for *N*,*N*-dimethylformamide. The microsolvated ions were also fully optimised, starting from the appropriately modified gas-phase structures; however, there is no guarantee that global minima have been located. All Jaguar calculations were carried out in Bristol. $^{15}N-^{15}N$ spin–spin NMR coupling constants[60] were computed using the ADF 2002 program package,[49] installed on computers of the UK Computational Chemistry Facility. These calculations were carried out at the gas-phase B3LYP geometries, using the standard BP86 functional, with no frozen electrons. Flexible Slater DZP basis sets were used on C, H and O, whereas the very large TZ2P basis was used on the N atoms so as to describe the core region as well as possible. High-accuracy grids and convergence thresholds were used throughout. The paramagnetic and diamagnetic orbital terms, as well as the electron-spin dependent Fermi-contact terms were included; the latter is by far the most important. Test calculations showed that the spin–dipole term was unimportant and it was therefore omitted.

Acknowledgement

The important intellectual contributions of Professor Roger W. Alder (Bristol), Professor Gary R. Weisman (University of New Hampshire, USA), Professor John White (Melbourne, Australia) and Drs. Frederick R. Manby and Jonathan P. H. Charmant (Bristol) to this and our earlier work in this area are very gratefully acknowledged. G.C.L.-J. thanks the Royal Society of Chemistry for unrestricted funding in the form of the Hickinbottom Fellowship. Pfizer Ltd and the Zeneca Strategic Research Fund made generous donations and the Nuffield Foundation provided a start-up grant (SCI/180/96/142). R.L.W. thanks Pfizer Ltd for a vacation bursary and for support in the form of a CASE award.

[1] G. A. Jeffrey, in *An Introduction to Hydrogen Bonding*, Oxford University Press, NY & Oxford, **1997**, pp. 11–32.
[2] a) W. W. Cleland, M. M. Kreevoy, *Science* **1994**, *264*, 1887; b) J. A. Gerlt, M. M. Kreevoy, W. W. Cleland, P. A. Frey, *Chem. Biol.* **1997**, *4*, 259.
[3] J. P. Guthrie, *Chem. Biol.* **1996**, *3*, 163.
[4] For leading references see: a) C. L. Perrin, B. K. Ohta, *J. Mol. Struct.* **2003**, *644*, 1; b) A. S. Mildvan, M. A. Massiah, T. K. Harris, T. G. Marks, D. H. T. Harrison, C. Viragh, P. M. Reddy, I. M. Kovach, *J. Mol. Struct.* **2002**, *615*, 163; c) K. S. Kim, D. W. Kim, J. Y. Lee, P. Tarakeshwar, K. S. Oh, *Biochemistry* **2002**, *41*, 5300; d) A. J. Mulholland, P. D. Lyne, M. Karplus, *J. Am. Chem. Soc.* **2000**, *122*, 534; e) A. Warshel, A Papazyan, *Proc. Natl. Acad. Sci. USA* **1996**, *93*, 13665.
[5] R. W. Alder, P. S. Bowman, W. R. S. Steele, D. R. Winterman, *J. Chem. Soc. Chem. Commun.* **1968**, 723.
[6] a) H. A. Staab, T. Saupe, *Angew. Chem.* **1988**, *100*, 895; *Angew. Chem. Int. Engl. Ed.* **1988**, *27*, 865; b) V. Raab, J. Kipke, R. M. Gschwind, J. Sundermeyer, *Chem. Eur. J.* **2002**, *8*, 1682.
[7] P. Hodgson, G. C. Lloyd-Jones, M. Murray, T. M. Peakman, R. L. Woodward, *Chem. Eur. J.* **2000**, *6*, 4451.
[8] C. L. Perrin, B. K. Ohta, *J. Am. Chem. Soc.* **2001**, *123*, 6520.
[9] M. Peräkylä, *J. Org. Chem.* **1996**, *61*, 7420.
[10] S. T. Howard, J. A. Platts, *J. Org. Chem.* **1998**, *63*, 3568.
[11] P. R. Mallinson, K. Wozniak, C. C. Wilson, K. L. McCormack, D. S. Yufit, *J. Am. Chem. Soc.* **1999**, *121*, 4640.
[12] I. Alkorta, J. Elguero, *Struct. Chem.* **2000**, *11*, 335.
[13] H. H. Limbach, *Magn. Reson. Chem.* **2001**, *39*, S1.
[14] For an introduction to scalar coupling across hydrogen bonds see: A. J. Dingley, F. Cordier, S Grzesiek, *Concepts Magn. Reson.* **2001**, *13*, 103.
[15] a) A. J. Dingley, S. Grzesiek, *J. Am. Chem. Soc.* **1998**, *120*, 8293; b) A. J. Dingley, J. E. Masse, R. D. Peterson, M. Barfield, J. Feigon, S. Grzesiek, *J. Am. Chem. Soc.* **1999**, *121*, 6019.

[16] K. Pervushin, A. Ono, C. Fernandez, T. Szyperski, M. Kainosho, K. Wüthrich, *Proc. Natl. Acad. Sci. USA* **1998**, *95*, 14147.

[17] H. Benedict, I. G. Shenderovich, O. L. Malkina, V. G. Malkin, G. S. Denisov, N. S. Golubev, H. H. Limbach, *J. Am. Chem. Soc.* **2000**, *122*, 1979.

[18] M. Pietrzak, J. Wehling, H. H. Limbach, N. S. Golubev, C. Lopez, R. M. Claramunt, J. Elguero, *J. Am. Chem. Soc.* **2001**, *123*, 4338.

[19] J. E. Del Bene, R. J. Bartlett, *J. Am. Chem. Soc.* **2000**, *122*, 10480.

[20] J. E. Del Bene, S. A. Perera, R. J. Bartlett, *Magn. Reson. Chem.* **2001**, *39*, S109.

[21] D. L. Bryce, R. E. Wasylishen, *J. Biomol. NMR* **2001**, *19*, 371.

[22] J. P. H. Charmant, G. C. Lloyd-Jones, T. M. Peakman, R. L. Woodward, *Tetrahedron Lett.* **1998**, *39*, 4733.

[23] J. P. H. Charmant, G. C. Lloyd-Jones, T. M. Peakman, R. L. Woodward, *Eur. J. Org. Chem.* **1999**, 2501.

[24] A. F. Pozarhski, A. N. Suslov, N. M. Starshikov, L. L. Popova, N. A. Klyuev, V. A. Adanin, *Zh. Org. Khim.* **1980**, *16*, 2216.

[25] A combination of trifluoroacetic anhydride (TFAA) and $K^{15}NO_3$ in $CHCl_3$ has been reported by Elguero et al., for the mono-^{15}N nitration of naphthalene.[55] We employed $Na^{15}NO_3$ instead of $K^{15}NO_3$ without noticeable effect on yield or rate.

[26] Since we required the dinitronaphthalene (**7**) we tested various other methods for effecting the second nitration without resort to use of a large excess of ^{15}N source. Suspecting that the mixed anhydride $CF_3CO_2{}^{15}NO_2$ generated from $K(Na)^{15}NO_3$/TFAA was not electrophilic enough to effect a second nitration, we instead used a mixture of TFA and TFAA. Together with a further one equivalent of $Na^{15}NO_3$ this effected a smooth double nitration (87% based on $Na^{15}NO_3$) in one pot.

[27] Both [$^{15}N_2$]-**3** and [$^{15}N_2$]-[**3**H]$^+$ exist as a mixture MESO and DL isomers which, because of their rapid interconversion at the NMR time-scale, were not analysed separately. The small quantities of [$^{15}N_2$]-**3** obtained (3.8% yield) and its rather air sensitive nature resulted in the ^{13}C NMR spectrum of the protonated form, [$^{15}N_2$]-[**3**H]$^+$, being rather unsuitable for simulation of the ABX portion due to the presence of decomposition products from [$^{15}N_2$]-**3** prior to protonation. The values obtained by simulation are given in Table 3.

[28] We were unable to locate a commercial source of anhydrous HI solution. Instead it was prepared in situ by metathesis of excess NaI with HCl in MeCN (in which NaI is fairly soluble but NaCl is not) and then precipitation of excess NaI by addition of diethyl ether.

[29] It is noted that as the isotope shift becomes negligible, the spectra tend towards an AA′X appearance (see for example use of a 0 ppb isotope shift under parameters "E" in Figure 1 upper section). However, this has no impact on extraction of J_{AB} if a full band-shape analysis (rather than frequency based approach) is employed. Consequently, statements that "it is impossible to measure $^{2H}J_{AB}$ under the conditions where the two atoms A and B are equivalent"[42] are not always correct. As the isotope effect increases substantially the X part of the spectrum cannot be used to extract J_{AB}. However, such large (and unrealistic) isotope shifts (see for example use of a 500 ppb isotope shift under parameters "A" in Figure 1 upper section) would result in sufficient chemical shift difference in the AB spin system that J_{AB} could be determined by full bandshape analysis of the ^{13}C satellites in the $^{15}N\{^1H\}$NMR spectrum.

[30] However, $\Delta^{2H}J_{NN}$, the change in the scalar N,N coupling upon protonation, does correlate approximately linearly with pK_a: $pK_a(MeCN) = 0.71(\pm 0.08)[(^{2H}J_{NN}[\mathbf{X}H]^+) - (^{2H}J_{NN}\mathbf{X})] + 12(\pm 0.3)$. It is noted that this correlation does not have an even spread of data points and may thus be coincidental. Nonetheless, the correlation is at least consistent with the lack of a stabilising hydrogen bond in **6** being responsible for the high pK_a of [**6**H]$^+$.

[31] Unlike C(1,8) in **6** which are simple doublets in the $^{13}C\{^1H\}$ NMR spectrum due to negligible N-N coupling, the methyl carbons in **6** are double doublets with the larger coupling (ca. 8 Hz) arising from ^1J(C,N) and the smaller coupling (ca. 0.8 Hz) arising from J(C,N′). It was earlier suggested that this coupling arises through hydrogen bonding of one of the methyl protons with the neighbouring N centre—as suggested by a solid state (X-ray) structure—and is thus a ^{2H}J(C,N) type coupling.[18] However, in solution such interaction (if present at all) is transient as it is well known that enantiotopic methyl groups in **6** (see R. W. Alder, J. E. Anderson, *J. Chem. Soc. Perkin Trans. 2* **1974**, 2086) and analogous systems[23] undergo rapid interconversion at the NMR time scale. We suggest that instead, this phenomenon arises from a through-space coupling brought about by the time-average proximity of the carbon and nitrogen centres during rapid interconversion of enantiomeric forms of **6**.

[32] A. J. Dingley, J. E. Masse, J. Feigon, S. Grzesiek, *J. Biomol. NMR* **2000**, *16*, 279.

[33] M. Hennig, J. R. Williamson, *Nucleic Acids Res.* **2000**, *28*, 1585.

[34] K. Pervushin, C. Fernandez, R. Riek, A. Ono, M. Kainosho, K. Wüthrich, *J. Biomol. NMR* **2000**, *16*, 39.

[35] A. Majumdar, A. Kettani, E. Skripkin, D. J. Patel, *J. Biomol. NMR* **1999**, *15*, 207.

[36] M. Hennig, B. H. Geierstanger, *J. Am. Chem. Soc.* **1999**, *121*, 5123.

[37] J. E. Del Bene, M. J. T. Jordan, *J. Phys. Chem. A* **2002**, *106*, 5385.

[38] J. E. Del Bene, S. A. Perera, R. J. Bartlett, *J. Am. Chem. Soc.* **2000**, *122*, 3560.

[39] J. E. Del Bene, S. A. Perera, R. J. Bartlett, *J. Phys. Chem. A* **2001**, *105*, 930.

[40] V. Sychrovsky, J. Vacek, P. Hobza, L. Zidek, V. Sklenar, D. Cremer, *J. Phys. Chem. B* **2002**, *106*, 10242.

[41] M. Pecul, J. Sadlej, *Chem. Phys. Lett.* **2002**, *360*, 272.

[42] M. Pietrzak, H. H. Limbach, M. Perez-Torralba, D. Sanz, R. M. Claramunt, J. Elguero, *Magn. Reson. Chem.* **2001**, *39*, S100.

[43] S. P. Brown, M. Perez-Torralba, D. Sanz, R. M. Claramunt, L. Emsley, *Chem. Commun.* **2002**, 1852.

[44] a) F. H. Allen, W. D. S. Motherwell, *Acta Crystallogr. Sect. B Struct. Sci.* **2002**, *58*, 407; b) A. G. Orpen, *Acta Crystallogr. Sect. B Struct. Sci.* **2002**, *58*, 398; c) F. H. Allen, *Acta Crystallogr. Sect. B Struct. Sci.* **2002**, *58*, 380.

[45] R. W. Alder, *Chem. Rev.* **1989**, *89*, 1215.

[46] a) The chemical shift of the ^{13}C NMR signals of C(1,8) in naphthalene was taken as 128.3 ppm and thus 256.6 ppm was subtracted from [$\Sigma^{13}C_{1,8}$] for each compound. b) H. Günther, in *NMR spectroscopy*, 2nd ed., Wiley, Chichester (UK), **1995**.

[47] R. W. Alder, P. Eastment, N. M. Hext, R. E. Moss, A. G. Orpen, J. M. White, *J. Chem. Soc. Chem. Commun* **1988**, 1528.

[48] R. W. Alder, *Tetrahedron* **1990**, *46*, 683.

[49] ADF2002.01, SCM, Theoretical Chemistry, Vrije Universiteit, Amsterdam, The Netherlands, http://www.scm.com

[50] See, however, for similar calculations on $^1J_{CH}$ and $^2J_{CXH}$ including continuum solvent: L. Sychrovsky, B. Schneider, P. Hobza, L. Zidek, V. Sklenar, *Phys. Chem. Chem. Phys.* **2003**, *5*, 734.

[51] C. J. Cramer, D. G. Truhlar, *Chem. Rev.* **1999**, *99*, 2161.

[52] For a discussion of microsolvation models and some leading references, see D. Sicinska, P. Paneth, D. G. Truhlar, *J. Phys. Chem. B* **2002**, *106*, 2708.

[53] For previous calculations on solvent effects on spin–spin coupling using microsolvated models, see ref. [50] and a) J. Autschbach, T. Ziegler, *J. Am. Chem. Soc.* **2001**, *123*, 3341; b) J. Autschbach, T. Ziegler, *J. Am. Chem. Soc.* **2001**, *123*, 5320.

[54] NBO 4, M. E. D. Glendening, J. K. Badenhoop, A. E. Reed, J. E. Carpenter, F. Weinhold, Theoretical Chemistry Institute, University of Wisconsin, Madison, WI, **1999**.

[55] S. J. Wilkens, W. M. Westler, J. L. Markley, F. Weinhold, *J. Am. Chem. Soc.* **2001**, *123*, 12026.

[56] W. D. Arnold, E. Oldfield, *J. Am. Chem. Soc.* **2000**, *122*, 12835.

[57] C. Lopez, P. Lorente, R. M. Claramunt, J. Marin, C. Foces-Foces, A. L. Llamas-Saiz, J. Elguero, H. H. Limbach, *Phys. Chem. Chem. Phys.* **1998**, *1*, 414.

[58] H. H. Hodgson, J. S. Whitehurst, *J. Chem. Soc* **1945**, 202

[59] *Jaguar v4.1*, Schrödinger, Inc., Portland, OR (USA), **1996**, **2001**.

[60] J. Autschbach, T. Ziegler, *J. Chem. Phys.* **2000**, *113*, 936.

Received: February 26, 2003 [F4890]

